Science of the Total Environment 906 (2024) 167159

Contents lists available at ScienceDirect

Science of the Total Environment

journal homepage: www.elsevier.com/locate/scitotenv

Identification of volatile organic compounds and their sources driving ozone and secondary organic aerosol formation in NE Spain

Marten in 't Veld [a,b,*], Roger Seco [a], Cristina Reche [a], Noemi Pérez [a], Andres Alastuey [a], Miguel Portillo-Estrada [c], Ivan A. Janssens [c], Josep Peñuelas [d,e], Marcos Fernandez-Martinez [c,d,e], Nicolas Marchand [f], Brice Temime-Roussel [f], Xavier Querol [a], Ana Maria Yáñez-Serrano [a,d,e]

[a] Institute of Environmental Assessment and Water Research, IDAEA-CSIC, 08034 Barcelona, Spain
[b] Department of Civil and Environmental Engineering, Universitat Politècnica de Catalunya, 08034 Barcelona, Spain
[c] PLECO (Plants and Ecosystems), Department of Biology, University of Antwerp, Wilrijk, Belgium
[d] CREAF, E08193 Bellaterra (Cerdanyola del Vallès), Catalonia, Spain
[e] CSIC, Global Ecology Unit, CREAF-CSIC-UAB, E08193 Bellaterra (Cerdanyola del Vallès), Catalonia, Spain
[f] Aix Marseille Univ., CNRS, LCE, Marseille, France

HIGHLIGHTS

- Five common sources were found for VOCs in BCN and MSY.
- The traffic and industry source was the biggest driver of OFP and SOAP in BCN.
- The OFP and SOAP at MSY was mostly driven by biogenic sources during summer.
- The SOAP was considerably lower in MSY (63 to 82 % difference).
- The OFP was similar in BCN and MSY in summer, but in winter the contrast was huge.

GRAPHICAL ABSTRACT

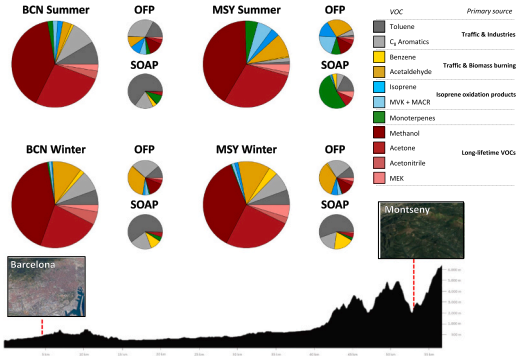

ARTICLE INFO

Editor: Anastasia Paschalidou

Keywords:
VOC
PTR-MS
Source apportionment
PMF
OFP
SOAP

ABSTRACT

Volatile organic compounds (VOCs) play a crucial role in the formation of ozone (O_3) and secondary organic aerosol (SOA). We conducted measurements of VOC ambient mixing ratios during both summer and winter at two stations: a Barcelona urban background station (BCN) and the Montseny rural background station (MSY). Subsequently, we employed positive matrix factorization (PMF) to analyze the VOC mixing ratios and identify their sources. Our analysis revealed five common sources: anthropogenic I (traffic & industries); anthropogenic II (traffic & biomass burning); isoprene oxidation; monoterpenes; long-lifetime VOCs. To assess the impact of these VOCs on the formation of secondary pollutants, we calculated the ozone formation potential (OFP) and secondary organic aerosol formation potential (SOAP) associated with each VOC. In conclusion, our study provides insights into the sources of VOCs and their contributions to the formation of ozone and SOA in NE Spain. The OFP was primarily influenced by anthropogenic aromatic compounds from the traffic & industries source at BCN

* Corresponding author at: Institute of Environmental Assessment and Water Research, IDAEA-CSIC, 08034 Barcelona, Spain.
E-mail address: marten.veld@idaea.csic.es (M. in 't Veld).

https://doi.org/10.1016/j.scitotenv.2023.167159
Received 30 May 2023; Received in revised form 30 August 2023; Accepted 15 September 2023
Available online 25 September 2023

(38–49 %) and during winter at MSY (34 %). In contrast, the summer OFP at MSY was primarily driven by biogenic contributions from monoterpenes and isoprene oxidation products (45 %). Acetaldehyde (10–35 %) and methanol (13–14 %) also made significant OFP contributions at both stations. Anthropogenic aromatic compounds originating from traffic, industries, and biomass burning played a dominant role (88–93 %) in SOA formation at both stations during both seasons. The only exception was during the summer at MSY, where monoterpenes became the primary driver of SOA formation (41 %). These findings emphasize the importance of considering both anthropogenic and biogenic VOCs in air quality management strategies.

1. Introduction

Volatile organic compounds (VOCs) play an important role in the formation of ozone (O_3) and secondary organic aerosol (SOA). O_3 is formed in the troposphere by photochemical reactions involving the oxidation of VOCs, including methane (CH_4) and carbon monoxide (CO) (Jacob, 1999a, 1999b). It has been estimated that approximately 90 % of global tropospheric O_3 is formed by the oxidation of VOCs (Jacob, 1999b; Jacob, 1999a; Möller, 2004; Stevenson et al., 2006; Young et al., 2013). Meanwhile, SOAs are primarily formed via the gas-to-particle conversion mechanism from precursor gases, which include VOCs, NH_3, H_2SO_4, HNO_3, and HCl, among others (Jacob, 1999c; Seinfeld and Pandis, 2016).

After the success of the EU policy for abating air pollutants, which caused a reduction in the ambient air concentrations of several (especially primary) pollutants, interest in secondary air pollutants has increased in both the science and policy realms. Notably, the ambient concentrations of secondary pollutants, such as O_3 and SOA, did not follow a decreasing trend (EEA, 2019, EEA, 2018a; EMEP/CCC, 2016; in 't Veld et al., 2021; Paoletti et al., 2014; Querol et al., 2016; Querol et al., 2014), which is detrimental to human health. The European Environmental Agency (EEA, 2021) reported 307,000 premature deaths in EU-28 countries attributable to fine particulate matter ($PM_{2.5}$) in 2019, 40,400 attributable to NO_2, and 16,800 attributable to O_3. Furthermore, O_3 also has a considerable negative effect on vegetation (Felzer et al., 2007; Krupa and Manning, 1988). It has been estimated that by 2030, there will be a global loss of €14–29 billion annually due to crop losses caused by O_3 (Avnery et al., 2011).

This is especially worrying for the western Mediterranean basin, which is prone to elevated O_3 levels due to low summer precipitation, high insolation, high NO_2 pollution, high biogenic VOC emissions, and the vertical recirculation of air masses caused by the combination of orographic features and meteorological patterns (Gangoiti et al., 2001; Millán, 2014; Millán et al., 2002; Millán et al., 1997; Pérez et al., 2004; Querol et al., 2017). Querol et al. (2016) reported that between 2000 and 2015, an O_3 level increase of 1.2 % yr^{-1} occurred at industrial and urban background sites in Spain, with an increase of 1.9 % yr^{-1} at traffic sites. Rural background concentrations did not show a significant trend but were higher in comparison to the other sites (urban, traffic, and industrial). Past studies have shown a relative increase in SOA throughout the study area. For example, Via et al. (2021) compared organic aerosol measurements using an aerosol chemical speciation monitor (ACSM) between May 2014 and May 2015, as well as between Sep 2017 and Oct 2018, showing an increase in the relative SOA content in PM_1 and a higher degree of oxidation during the latter period. The same observation was made by in 't Veld et al. (2021), who estimated relative SOA increases of 12 and 8 % in the chemical composition of $PM_{2.5}$ in urban and rural background stations, respectively, between 2009 and 2018. Furthermore, secondary pollutants are closely linked to one another since higher O_3 levels increase the readily available hydroxyl- and nitrate-oxidizing radicals ($OH^{\bullet}$ and $NO_3^{\bullet}$) in the urban atmosphere. An example of this was observed in downtown Madrid, where a 30–40 % increase in O_3 was measured alongside $OH^{\bullet}$ and $NO_3^{\bullet}$ increases of up to 70 and 90 %, respectively, between 2007 and 2014 (Saiz-Lopez et al., 2017). Additionally, a reduction in sulfur dioxide (SO_2) (EEA, 2015) and nitrogen oxides (NO_x) (EEA, 2018b) in Europe between 1990 and 2011 also led to a decrease in the consumption of the oxidizing radicals, which increased their availability and might have resulted in an atmosphere more prone to SOA production (Querol et al., 2018; Saiz-Lopez et al., 2017).

Increased knowledge regarding the relationships of VOC sources and their potential to form O_3 and SOA is required to develop cost-effective abatement strategies in the western Mediterranean. VOCs encompass a wide variety of organic compounds, which include over 1000 chemical components originating from a variety of sources. Although previous studies have investigated the VOCs occurring in NE Spain (Filella and Peñuelas, 2006; Seco et al., 2013; Seco et al., 2011; Yáñez-Serrano et al., 2021a) and contributed to a greater understanding of the VOCs in this region, source apportionment was only performed in a rural background site during summer (Yáñez-Serrano et al., 2021a), while a comparison between an urban background and rural background was only performed during winter (Seco et al., 2013). Finally, most published studies have not investigated the potential of existing VOCs to form O_3 or SOA.

This study focuses on evaluating the levels and source contributions of VOCs in NE Spain by using proton-transfer-reaction mass spectrometry (PTR-MS) to measure online VOC mixing ratios. This allowed us to identify and quantify a selection of VOCs in both the Barcelona urban background site and the Montseny rural background site. The differences between the stations allowed us to highlight differences between an urban and rural environment and show which VOCs are emitted locally and which are emitted regionally. Furthermore, the extensive measurements conducted during both the summer and winter months at both stations allowed us to identify seasonal patterns. The use of both the O_3 formation potential (OFP) and the SOA formation potential (SOAP) to estimate the amount of O_3 and SOAs that VOCs can form under ideal situations, respectively, permits the identification of the most potentially important precursors to both O_3 and SOA formation in the study area. Additionally, to aid in the identification of VOC sources, a positive matrix factorization (PMF) model was applied on the VOC dataset to obtain the sources.

2. Methodology

2.1. Sampling location

VOC measurements were performed using PTR-MS at two stations in the conurbation of Barcelona in NE Spain. Both sites are included in the European Aerosols, Clouds, and Trace Gases Research Infrastructure Network (ACTRIS) and the Air Quality Monitoring Network (AQMN) of the Catalan Government, while MSY is part of the Global Atmosphere Watch (GAW) network of the World Meteorological Organization (WMO) (Fig. 1). A mountain in the Montseny Natural Park, located in El Vilar de la Castanya (el Brull), is home to one of the two stations, which is a rural background station (hereafter MSY; 41°46′45.63"N, 02°21′28.92"E; 720 m a.s.l.). The MSY station is located 40 km from the Mediterranean coast and 50 km to the N-NE of Barcelona. It has been demonstrated to be representative of the regional ambient background and is sufficiently elevated and distant from specific urban anthropogenic emission sources (Cusack et al., 2012; in 't Veld et al., 2023; in 't Veld et al., 2021; Pandolfi et al., 2016; Pandolfi et al., 2014; Pérez et al., 2008; Pey et al., 2009; Ripoll et al., 2015), although the station may be impacted by emissions from urban and industrial areas during

anticyclonic atmospheric conditions due to wind circulation (Ealo et al., 2018; Gangoiti et al., 2001; Millán et al., 2002; Millán et al., 1997; Pandolfi et al., 2016; Pandolfi et al., 2013). The second station is an urban background air quality station (hereafter BCN; 41°23′14.5"N 2°06′55.6″E; 68 m asl) located at the Institute of Environmental Assessment and Water Research (IDAEA-CSIC) in Barcelona. It is positioned adjacent to Diagonal Avenue, one of the city's main roads, and is flanked by a variety of commercial activities (Amato et al., 2009; Cusack et al., 2012; in 't Veld et al., 2023; in 't Veld et al., 2021; Pandolfi et al., 2016; Pandolfi et al., 2014; Pérez et al., 2008; Pey et al., 2009; Querol et al., 2014, Querol et al., 2004a, b; Ripoll et al., 2015). At both measurement sites, an aethalometer (Magee Scientific, USA, model AE33) was used to quantify the aerosol light absorption coefficient at seven different wavelengths (370, 470, 520, 590, 660, 880, and 950 nm) and the mass concentration of black carbon (BC) (Drinovec et al., 2015). Additionally, the AQMN used instrumentation to measure hourly concentrations of O_3, CO, NO, NO_2, and NO_x (Table S6). The results of the gas data are shown in Fig. 2 and discussed in Section 2 of the SI. Finally, ambient temperature and solar radiation were measured at the station in MSY, and at the Department of Physics building of the Barcelona University for the BCN station. Wind speed and direction data were also usually included; however, this was unavailable at MSY during the 2022 measurement period and is thus not discussed in this paper.

2.2. PTR-MS sampling

The VOC mixing ratios in ambient air were measured using PTR-MS. Different instruments were used depending on the location and year. In 2022, a time-of-flight mass spectrometer (PTR-ToF-MS, Ionicon PTR TOF 4000X2, Ionicon Analytik, Innsbruck, Austria) was used in Barcelona, while a PTR-MS with a quadrupole mass spectrometer (PTR-MS, Ionicon PTR-MS Quad, Ionicon Analytik, Innsbruck, Austria) was used at MSY. The measurements at MSY in 2017 used a PTR-ToF-MS (Ionicon PTR TOF 8000, Ionicon Analytik, Innsbruck, Austria). A detailed description of the instrument is provided by Graus et al. (2010). In summary, proton transfer is a form of soft chemical ionization from hydronium ions (H_3O^+), with the distinct feature that H_3O^+ ionizes compounds with little energy excess, resulting in minor fragmentation, thus making it an excellent method to measure ambient air (de Gouw et al., 2003; Dunne et al., 2018; Ionicon Analytik GmbH, 2014; Warneke et al., 2011). The parameters of each PTR-MS are described in Table 1. For the 2022 measurements, a periodic calibration was made during the measurements, with automatic blanks taken every hour for MSY and every 6 h for BCN. For the measurement in 2017, a calibration was performed at the start of the measurement. Since a blank measurement was missing for the measurement period, an approximation of the blank was made using blanks from the previous campaign using the same

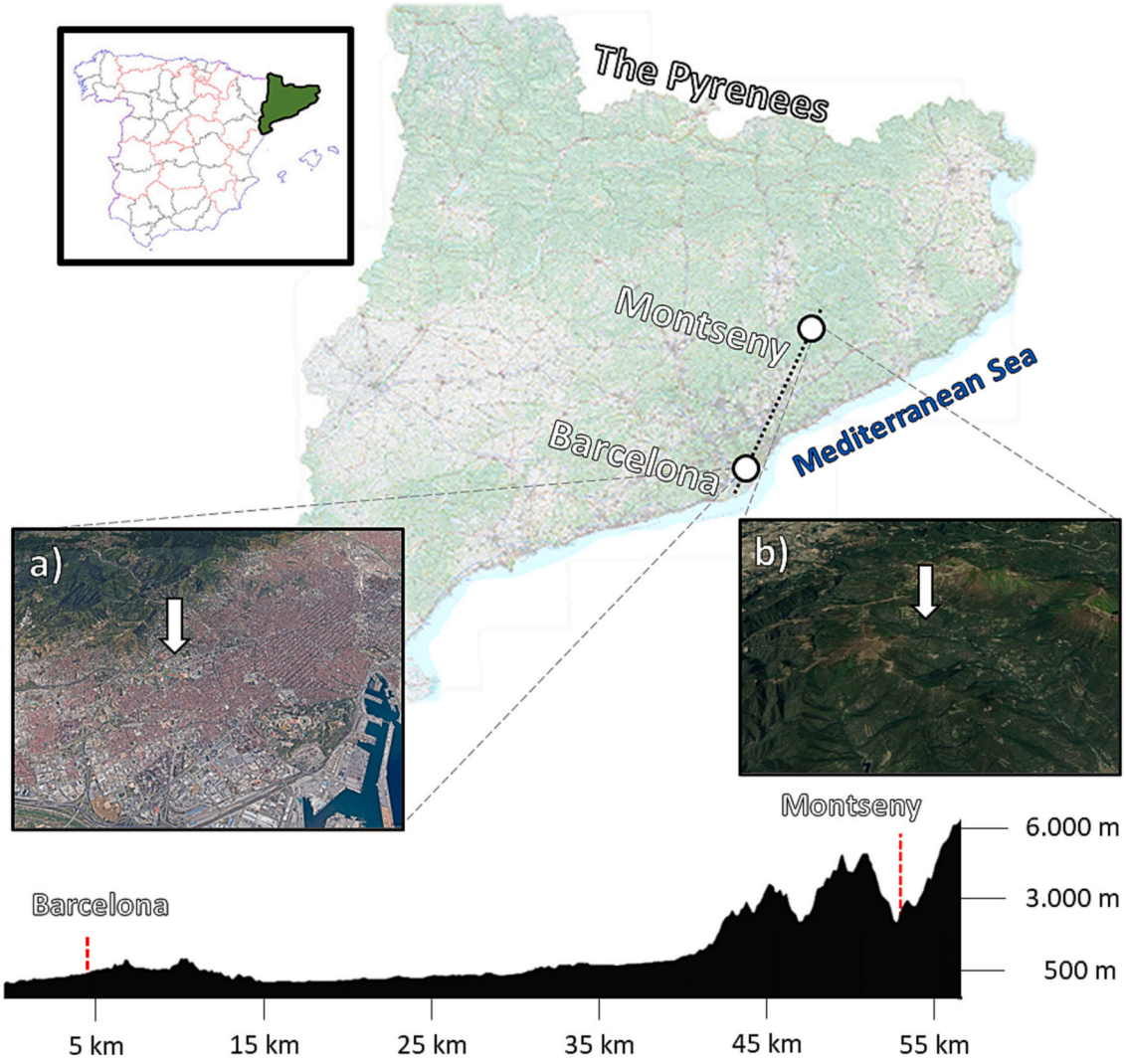

Fig. 1. Locations of the measurement stations in Catalonia, NE Spain. a) location of the Barcelona urban (BCN) station (41°23′14.5"N 2°06′55.6″E, 68 m a.s.l.). b) location of the Montseny rural (MSY) station (41°46′45.63"N, 02°21′28.92″E, 720 m a.s.l.). Altitude profile between BCN and MSY is presented at the bottom. Images credits: ©Google Earth and Institut Cartogràfic i Geològic de Catalunya (ICGC).

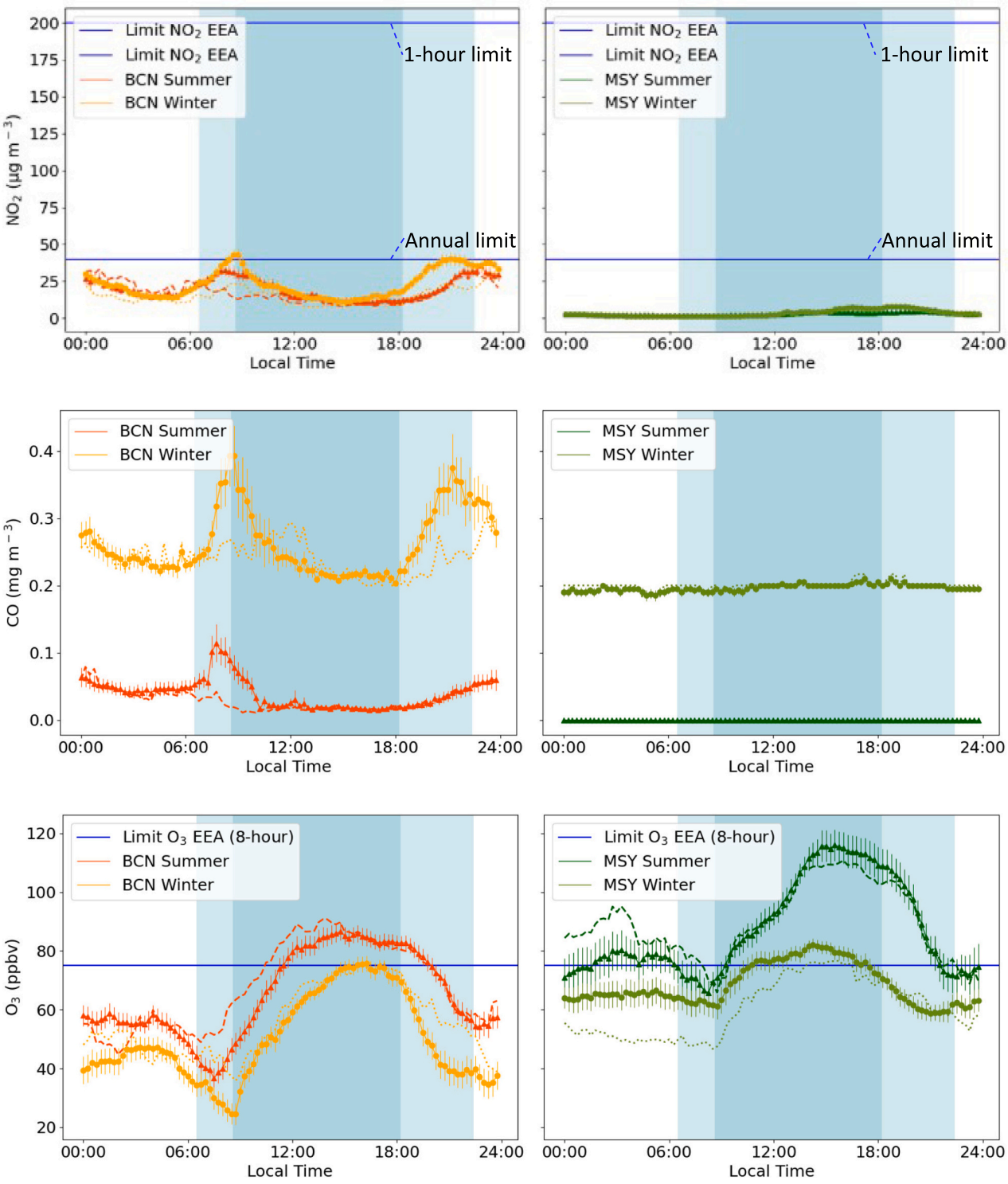

Fig. 2. Mean diel variation of 15-minute averaged NO_2 (top), CO (middle), and O_3 (bottom) concentrations using the same days as the VOC measurements. Dotted lines represent the weekend diel variation. Blue lines represent the current EU air quality standards (EC, 2008) set for 8-hour averages (O_3), 1-hour averages (NO_2), or annual averages (NO_2). The CO cycles in MSY could not show a diel variation due to low accuracy. The CO 8-hour average limit is 10 mg m^{-3}, which is far above the scale of this plot and, thus, is not shown here. A dark blue background represents daylight hours during winter (February–March), while blue background represents daylight during summer (May–June).

apparatus. Table 1 presents the measurement periods at both stations, the apparatus used, and the measurement frequency. The periods were selected as approximately 1 month in duration when data were available at both BCN and MSY.

Two gravimetrically prepared multicomponent standards created by Apel-Riemer (Apel-Riemer Environmental Inc., Miami, USA) and Restek (Restek Corporation, Bellefonte, PA, USA) contained all VOC compounds discussed here, which were humidity-dependent calibrated at various dilution steps. These calibrations used bubbled zero air to dilute the standards and were regulated as closely as possible to the ambient humidity. A list of the compounds is presented in Table 2. Notably, since PTR-MS measures the exact masses of compounds, it is not compound-

Table 1
Measurement periods of the study, with the apparatus used, dates, and measurement frequency.

Station	Period	Instrument	Start Date	End Date	Frequency
Barcelona	Winter	PTR-ToF-MS 4000X2	08 Feb 2022	07 Mar 2022	10 s
Barcelona	Summer	PTR-ToF-MS 4000X2	23 May 2022	27 Jun 2022	10 s
Montseny	Winter	PTR-MS Quad	17 Feb 2022	02 Mar 2022	25 s
Montseny	Summer	PTR-MS Quad	31 May 2022	14 Jun 2022	25 s
Montseny	2017	PTR-ToF-MS 8000	22 Jun 2017	20 Jul 2017	3 min

Table 2
List of calibrated compounds for the PTR-Quad-MS and PTR-ToF-MS with the mass-to-charge (*m/z*), average limit of detection (LoD), and median uncertainty (%).

m/z	Compound calibrated	Compound attributed	LoD PTR-Quad-MS	LoD PTR-ToF-MS	Uncertainty
33	Methanol	Methanol	1.98	0.13	17 %
42	Acetonitrile	Acetonitrile	0.07	0.01	18 %
45	Acetaldehyde	Acetaldehyde	0.16	0.09	10 %
59	Acetone	Acetone Propanal	0.17	0.04	8 %
69	Isoprene	Isoprene Furan (Quad-MS) MBO fragment	0.16	0.05	12 %
71	Methyl vinyl ketone	Methyl vinyl ketone Methacrolein	0.12	0.01	11 %
73	Methyl ethyl ketone	Methyl ethyl ketone	0.10	0.02	11 %
79	Benzene	Benzene	0.06	0.01	9 %
93	Toluene	Toluene	0.18	0.01	6 %
107	Ethylbenzene	C_8 aromatics	0.42	0.01	7 %
107	*o*-, *m*-, *p*-xylene				
137	α-Pinene	Monoterpenes	0.05	0.01	12 %

specific since compounds with the same masses may interfere with the measured signal. The compounds were assigned to the masses based on their exact mass, the compounds included in the calibration canister, the GLOVOCs database (Yáñez-Serrano et al., 2021b), and previous measurements in the study area (Peñuelas et al., 2009; Seco et al., 2013; Seco et al., 2011; Yáñez-Serrano et al., 2021a). Nevertheless, some other compounds might contribute to these masses during ambient measurement. While most masses had a single compound assigned to them, a few masses had multiple compounds assigned to them. A mass-to-charge ratio (*m/z*) of 59 is the same for both acetone and propanal. However, the ambient concentrations of propanal are significantly lower when compared to acetone (Hellén et al., 2004; Li et al., 2018). Therefore, in this study, most instances of m/z 59 will be assumed to be acetone. A similar situation occurred with m/z 69, which was primarily attributed to isoprene but has possible interference from furan and fragments of 2-methyl-3-butene-2-ol (MBO); however, these concentrations are much lower when compared to isoprene. Therefore, m/z 69 will be assumed to be isoprene in this study (Juráň et al., 2017; Karl et al., 2012; Kaser et al., 2013). Meanwhile, m/z 71 can be both methyl vinyl ketone (MVK) and methacrolein (MACR) since both are isomers of C_4H_6O. Therefore, this mass was considered to be a combination of these two VOCs. Moreover, m/z 107 can be either ethylbenzene, *o*-, *p*-, or *m*-xylene, and is thus referred to as C_8 aromatics since they are all isomers of C_8H_{10}. Another common VOC with m/z 107 is benzaldehyde (C_7H_6O). While benzaldehyde has a different exact mass and can be distinguished using PTR-ToF-MS, it cannot be ruled out that it interferes with the C_8 aromatics peak when using quadrupole-based PTR-MS instruments. Finally, m/z 137 contains various monoterpenes that are isomers of $C_{10}H_{16}$ and are thus referred to as monoterpenes. The uncertainty of the measurements was calculated according to the error propagation approach (Doerffel, 1984). This method calculates the total uncertainty of the PTR-MS while considering the calibration uncertainty (which includes multicomponent gas standard and mass flow controller errors), the PTR-MS instrument, and the background error. Table 2 also reports the median uncertainty as a percentage, based on the uncertainty from the calibration gas, blanks, and measurements combined. Calculations of the ozone formation potential, SOA formation potential, and correlations are described in Section 1 of the SI.

2.3. PMF source apportionment

The source apportionment analysis was performed on the VOC dataset via PMF using the U.S. Environmental Protection Agency's PMF v5.0 software (Norris et al., 2014). PMF is a multivariate factor analysis tool that decomposes time trends in chemical composition into factor contributions and chemical profiles by performing chemical mass balance between measured species concentrations and the sum of source contributions for those species:

$$X_{ij} = \sum_{k=1}^{p} g_{ik} * f_{kj} + e_{ij}$$

Here, X is the data matrix with i number of samples and j number of chemical species. p is the number of sources, f is the chemical profile of each source with mass contribution g, and e_{ij} is the residual for each sample. To obtain better factor profiles, certain VOCs were set as "weak" species, which means that the uncertainty is tripled. These species were selected based on the signal-to-noise ratio ($0.5 > S/N > 1.5$) and visual anomalies in the factor profiles. Strong species included acetone, isoprene, benzene, toluene, and monoterpenes. Weak species included methanol, acetonitrile, acetaldehyde, MVK + MACR, methyl ethyl ketone (MEK), and C_8 aromatics.

In this study, a multisite solution was used by aggregating the BCN and MSY data into a single dataset. The main benefits of running a multisite PMF were the inclusion of a larger dataset when compared to separate single-site PMF models. A multisite PMF produces more robust results and can obtain source profiles common to both sites, thus allowing a direct comparison between the two stations. This has not been previously done for VOC measurements in the study area but has been successfully applied to the chemical speciation of particulate matter (in 't Veld et al., 2023; in 't Veld et al., 2021; Pandolfi et al., 2016). However, we also acknowledge the limitations of this analysis stemming from the physical distance between the two stations, possible differences in local source types and their magnitude, and different chemical profiles for the same types of sources (Escrig et al., 2009). The results were bootstrapped 100 times, and a displacement model was used to determine the uncertainties in the PMF results.

3. Results and discussion

3.1. VOC mixing ratios

Table 3 presents the 11 compounds, their masses, and their average (taken over the whole campaign, Section 3 of the SI) mixing ratios separated by season and station. A detailed description of the measure VOC species is described in Section 4 of the SI. In all cases (both at BCN and MSY during both seasons), methanol was the most abundant VOC, which mostly originated from biogenic emissions and secondary formation (Holzinger et al., 2005; Holzinger et al., 1999; Lewis et al., 2005; Seco et al., 2007; Sjostedt et al., 2012). Acetone was the second-most abundant VOC and, like methanol, mostly originated from biogenic emissions and secondary formation (Arnold et al., 2004; Holzinger et al.,

Table 3
Whole-campaign average mixing ratios of the 11 VOCs measured in this study, in parts per billion (ppbv), with the standard deviation. Data are separated by season and station. m/z standard for mass divided by charge.

Compound	m/z	Barcelona		Montseny	
		Winter	Summer	Winter	Summer
Methanol	33	3.50 ± 4.87	3.73 ± 3.58	1.46 ± 0.80	3.89 ± 1.67
Acetonitrile	41	0.41 ± 0.81	0.29 ± 0.59	0.10 ± 0.06	0.12 ± 0.05
Acetaldehyde	43	0.92 ± 0.86	0.31 ± 0.27	0.48 ± 0.28	0.84 ± 0.44
Acetone + propanal	59	1.93 ± 1.89	2.50 ± 2.14	1.02 ± 0.49	2.76 ± 1.04
Isoprene	69	0.04 ± 0.16	0.18 ± 0.16	0.05 ± 0.09	0.30 ± 0.42
MVK + MACR	71	0.09 ± 0.07	0.17 ± 0.15	0.05 ± 0.06	0.55 ± 0.50
MEK	73	0.22 ± 0.18	0.24 ± 0.21	0.19 ± 0.16	0.30 ± 0.18
Benzene	79	0.14 ± 0.20	0.08 ± 0.11	0.13 ± 0.08	0.04 ± 0.06
Toluene	93	0.47 ± 0.66	0.80 ± 1.00	0.22 ± 0.31	0.09 ± 0.10
C_8 aromatics	107	0.64 ± 1.02	0.87 ± 1.01	0.29 ± 0.38	0.15 ± 0.15
Monoterpenes	137	0.05 ± 0.07	0.19 ± 0.25	0.02 ± 0.02	0.45 ± 0.53

2005; Holzinger et al., 1999; Lewis et al., 2005; Seco et al., 2007; Singh et al., 1994; Sjostedt et al., 2012). The high levels of these short-chain oxygenated VOCs can be attributed to their low reactivity with atmospheric oxidants, especially when compared to the other set of VOCs (Table 6) (Arnold et al., 2004; Filella and Peñuelas, 2006; Lewis et al., 2005; Seco et al., 2013), which will be discussed in detail in subsequent sections.

The average mixing ratios of this study were compared to previous studies conducted in the study area between 2009 and 2019 (Section 5 of the SI). The comparison between these studies showed that the mixing ratios at MSY were stable between 2009 and 2019, indicating consistency in the regional air quality regarding VOCs. At BCN, differences were observed, where the different measurement periods and protocols used could have contributed to this. Additionally, since BCN was located closer to the sources in comparison to MSY, the measurements might be more prone to the variations of local sources from one campaign to another, especially regarding the mean values of short-period measurement campaigns.

In summer, all VOCs at MSY show a small peak in the evening (Fig. 3). This is a currently unknown anomaly of the MSY station, which was also observed in the temperature and radiation data. This phenomenon was also observed by Yáñez-Serrano et al. (2021a), who sampled VOCs a few kilometers from the measurement station, which indicates that this is not an anomaly of the measurement station.

It must be noted that the observed mixing ratios do not represent the initial mixing ratios of the VOCs due to photochemical losses, especially with high temperature and during O_3 episodes (Liu et al., 2023). Three studies in China compared the VOC source apportionment using both the observed and initial VOC mixing ratios, using a box model. While various factors were considerably underestimated, all three studies found the exact same amount of factor (Liu et al., 2023; Wu et al., 2023; Yang et al., 2022). Though, Gu et al. (2023) found that using the initial concentration managed to identify a separate, petrochemical enterprise source.

The underestimation due to photochemical loss impacts VOCs with relatively high reactivities. In the case of our study this would mostly involve the aromatic compounds, isoprene, and monoterpenes.

The studies show that alkenes are the group with the biggest photochemical loss. Liu et al. (2023) showed an underestimation of 73 % of biogenic sources, which was mostly traced by isoprene, while Gu et al. (2023) showed that isoprene had a 98.6 % photochemical loss during their study period. However, Wu et al. (2023) stated that using the xylene/ethylene ratio to calculate the initial VOC mixing ratios, which is the common way of calculating the initial VOC mixing ratios, would significantly overestimate the initial isoprene concentration. Using a sequential reaction model, using the photochemical products MVK and MACR, it was determined that isoprene was underestimated by over 50 % (Stroud et al., 2001).

Regarding aromatics Wu et al. (2023) estimated 13.1 % of the initial aromatic concentrations to be lost photochemically. This was mostly driven by toluene and xylenes, with a minor contribution from benzene and ethylbenzene. Gu et al. (2023) observed a 66.2 % loss of aromatic hydrocarbons, mostly driven by trimethylbenzene and styrene, but also toluene, xylene, and ethylbenzene to a lesser extent. Yang et al. (2022) calculated a 72.6 % photochemical loss from aromatics, with especially xylene, and toluene decreasing considerably. Liu et al. (2023) saw a much lower decrease in aromatics, with a 31.7 % decrease due to photochemical loss. This was primarily from xylenes, toluene, and styrene, followed by benzene and ethylbenzene. Other VOCs were less affected by photochemical loss. Thus an underestimation of biogenic and aromatic compounds is expected due to photochemical loss.

3.2. *Source apportionment*

To determine the sources of all VOCs, we performed a multisite PMF source apportionment. The model was applied to an aggregated dataset from both the summer and winter periods of both stations. This made it possible to compare source profiles between the different seasons and stations. The source apportionment analysis identified five factors (Table 4), with the profiles presented in Fig. 4. For ease of interpretation, all factor names are written in *italics* in this paper. The optimal number of sources was selected by inspecting the Q values, residuals, G space plots, and physical meanings of the factors. To confirm the optimal factor profiles of the PMF model, the data were also bootstrapped. Each dataset was bootstrapped 100 times with a minimum correlation R-value of 0.6. Finally, the model error was estimated using the base model displacement method.

- Factor 1: Anthropogenic I: traffic & industry factor
  - o This source originated from traffic and industry emissions at BCN and was mostly long-distance transport at MSY.
- Factor 2: Anthropogenic II: traffic & biomass burning factor
  - o Additional anthropogenic source that accounted for a second traffic source and biomass burning.
- Factor 3: Isoprene oxidation factor
  - o Contains isoprene and its oxidation products, which are both anthropogenic and biogenic at BCN, and mostly biogenic at MSY.
- Factor 4: Monoterpene factor
  - o A biogenic source at both stations that contained only monoterpenes.
- Factor 5: Long-lifetime VOC factor
  - o A source combining the VOCs with long atmospheric lifetimes. These were mostly anthropogenic at BCN, while biogenic and formed due to photo-oxidation at MSY. This source also contained VOCs that could not be attributed to the other four factors.

To confirm the findings of the multisite PMF, separate PMF analyses were performed for both the BCN and MSY stations, combining both seasons. All sources were identified in separate PMFs with the following notes. At MSY, the biogenic sources were identified as a single source combining isoprene, MVK + MACR, and monoterpenes. At BCN, the biogenic sources were separated into two different sources, as observed in the multisite solution. As will be described later in this section, this difference is due to the following factors. In the BCN area, isoprene can be emitted from biogenic and anthropogenic sources; however, such an

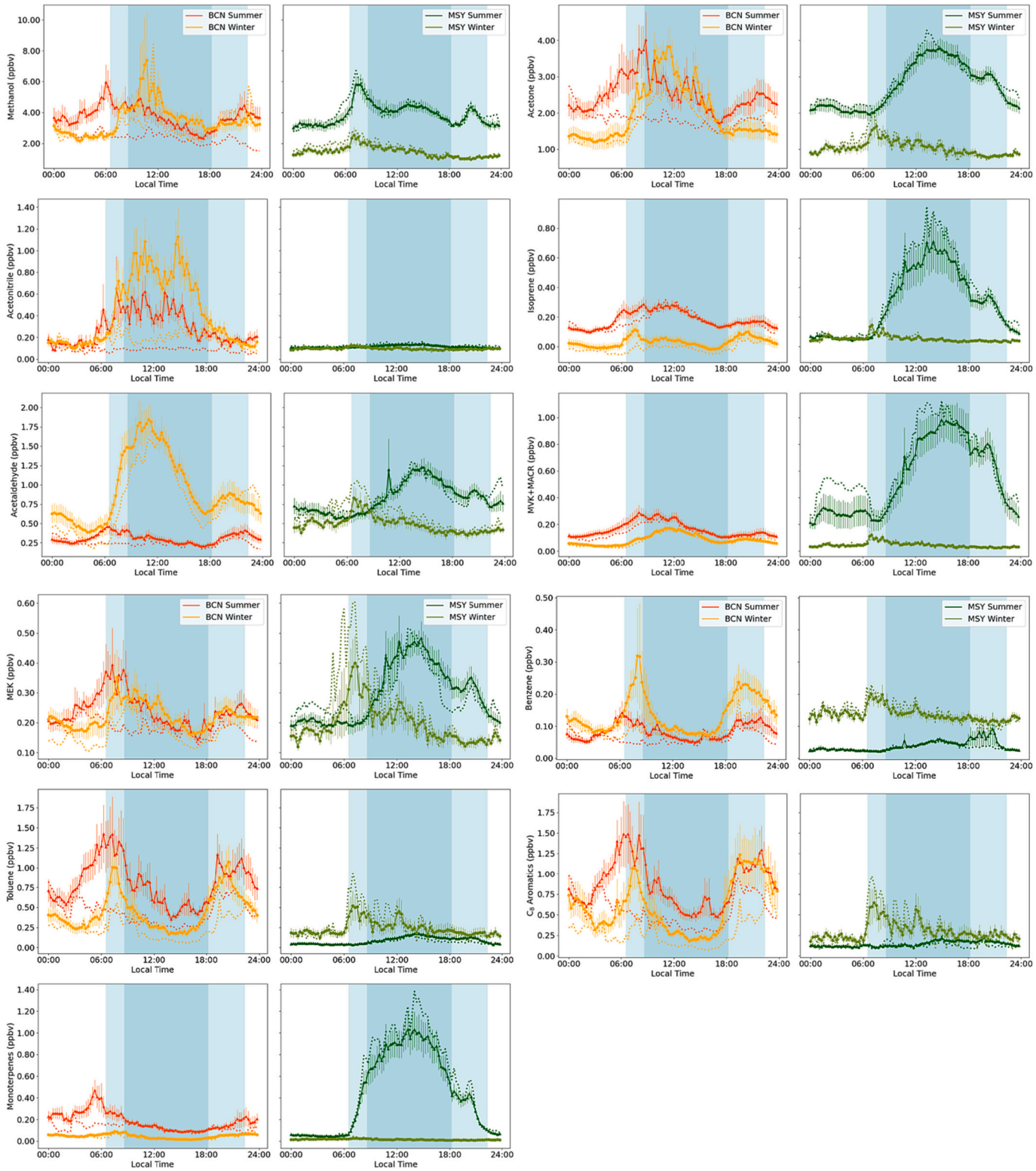

Fig. 3. Mean diel variation of the 15-minute average mixing ratios of all VOCs, with the respective standard deviations. Dotted lines represent the weekend diel variation. Orange: BCN Summer (May – June); Yellow: BCN Winter (February – March); Dark green: MSY Summer (May – June); Light green: MSY Winter (February – March). Dark blue background represents the daylight hours during winter, while blue background represents the daylight hours during summer.

anthropogenic source was negligible at MSY. Furthermore, the *long-lifetime VOC* factor was separated into two distinct groups at MSY, with one being characterized by photo-oxidized VOCs, which was lacking in the BCN PMF—and thus in the multisite PMF. All other sources were identified at both stations with the same tracers.

Table 4 reports the average mass contribution of each source factor. The long lifetime VOCs account for 46–61 % of the relative TVOC (Total VOC) mass, showing their high contribution to the atmospheric VOC mixing ratios due to their long lifetimes in the troposphere at both stations. Due to the variety of sources, this factor was quite similar between

Table 4
Whole-campaign average mixing ratios (ppbv) of the five multisite PMF sources, with the standard deviations.

Source	Barcelona		Montseny	
	Summer	Winter	Summer	Winter
Traffic & industry	2.47 ± 2.84	1.18 ± 1.96	0.00 ± 0.20	0.47 ± 0.93
Traffic & biomass burning	0.68 ± 0.87	1.97 ± 1.86	0.79 ± 0.68	2.20 ± 0.71
Isoprene oxidation	0.53 ± 0.46	0.20 ± 0.35	1.36 ± 1.72	0.17 ± 0.16
Monoterpenes	0.57 ± 0.85	0.12 ± 0.18	1.53 ± 1.72	0.02 ± 0.04
Long-lifetime VOCs	4.60 ± 3.39	4.44 ± 3.91	5.68 ± 1.61	2.46 ± 0.93

the summer and winter in BCN, but in MSY higher levels were found in the summer due to additional biogenic emissions. The *traffic & industry* source was the second most contributing source in BCN (15–28 %), while being very minor (0–9 %) in MSY due to the distance from traffic and industry sources. The *traffic & biomass* burning source had a relatively higher contribution to the relative TVOC at both stations, with 8 % during summer and 25–41 % during winter due to residential heating. The biogenic factors (*isoprene oxidation* and *monoterpenes*) were much higher in MSY compared to BCN due to its proximity to the sources. It is important to note however, that the masses of the other source factors are considerably underestimated due to photochemical loss from aromatic compounds, isoprene, and monoterpenes. Studies have shown a considerable underestimation of at least 50 % for isoprene, and an underestimation between 13.1 and 72.6 % for aromatics (Gu et al., 2023; Liu et al., 2023; Stroud et al., 2001; Wu et al., 2023; Yang et al., 2022). The mass concentration of the 5 factors (Table 4) therefore, overestimates the relative contribution of the long-lifetime VOC factor, which is the sole factor not containing aromatics or alkenes. The exact uncertainty cannot be determined, as it is very location and compound specific and depends strongly on the meteorological and oxidation circumstances. Though, the *long lifetime VOCs* would still be the factor with

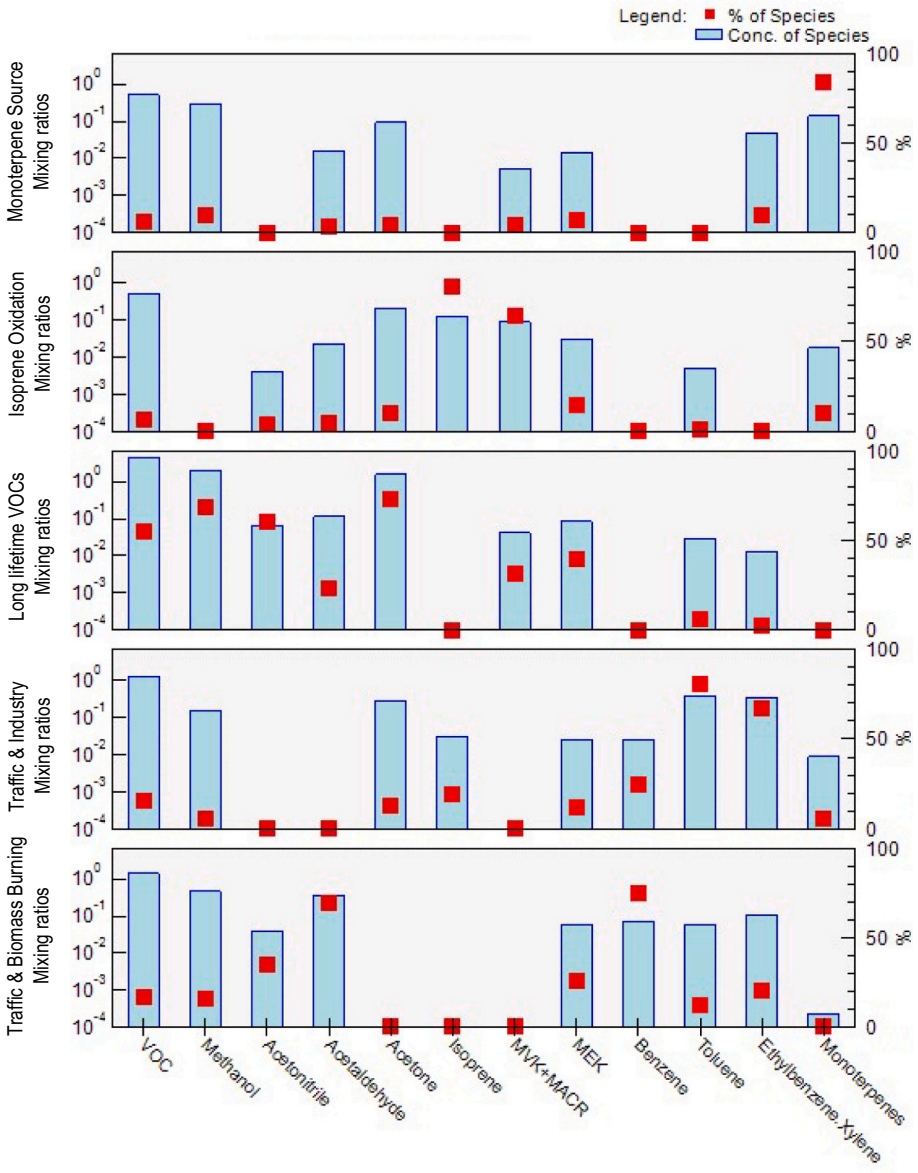

Fig. 4. Factor profiles of the PMF analysis using the complete multisite dataset of both seasons from both BCN and MSY. VOCs are presented on the bottom-axis; the mixing ratios (ppbv) of the VOC at the factor on the left-hand side vertical axis, presented in blue bars; the relative percentual contributions of each chemical species to said factor are shown as red squares on the right-hand side vertical -axis.

the biggest mass concentration, as even if all sources were increased by 70 %, which was the rough estimation of the photochemical loss reported by various papers (Gu et al., 2023; Liu et al., 2023; Stroud et al., 2001; Wu et al., 2023; Yang et al., 2022), it would still be the highest contributing source (except for MSY winter).

3.2.1. Factor 1: Anthropogenic I: Traffic & Industry

Factor 1 was mostly traced by toluene (81 % of the total toluene) and C_8 aromatics (67 %), with tracers of benzene (25 %) and isoprene (19 %, discussed in more detail in *Factor 3*). These VOCs are mostly emitted anthropogenic VOCs. The high content of aromatic hydrocarbons and oxygenated compounds without biogenic VOCs further indicates the anthropogenic origin of this factor.

The diel variation of BCN (Fig. 5) showed two clear traffic peaks during both seasons (8:00 and 20:00), coinciding with those of CO and NO_2 (Fig. 2). Previous studies at BCN determined that anthropogenic VOC emissions are primarily caused by road traffic (Filella and Peñuelas, 2006; in 't Veld et al., 2021; Jiménez et al., 2005). The lower concentrations during weekends further confirm this since anthropogenic emissions from traffic and industry are significantly lower during weekends when compared to weekdays. This phenomenon was also observed for CO and NO_2 (Filella and Peñuelas, 2006; in 't Veld et al., 2021). Moreover, these phenomena were also observed for the major constituents of this factor, toluene and C_8 aromatics (Fig. 3), indicating that they both drive this factor.

These observations point to the anthropogenic origin of this factor. The toluene to benzene (T/B) ratio furthermore confirms the anthropogenic origin of toluene and benzene. Generally, T/B ratios >8 or 10 are observed in industrial areas (Cui et al., 2022; Pinthong et al., 2022; Tan et al., 2021), while ratios ranging between 1.0 and 4.3 would indicate vehicle emissions as the primary source (Cui et al., 2022; Heeb et al., 2000; Khoder, 2007; Langford et al., 2009; Pinthong et al., 2022). If the T/B ratio fell below 1, the main source of emissions would come from biomass burning (Liu et al., 2008; Tan et al., 2021). In both stations, the T/B ratio was lower in the winter when compared to the summer (Fig. 6). At BCN, the T/B ratio was 9.73 ± 5.16 during summer, which indicates that BCN is dominated by industrial emissions mixed with traffic emissions since industrial emissions are characterized by low levels of benzene and high levels of toluene (Filella and Peñuelas, 2006; Seco et al., 2013). During winter, the T/B ratio was lower with 2.92 ± 2.28, which is in line with previous studies conducted in the study area (Filella and Peñuelas, 2006; Seco et al., 2013). The lower values during winter were also due to an increase in benzene emissions from residential heating, which will be discussed further in *Factor 2*. During both seasons, a decrease in the T/B ratio could be observed due to the substantial decrease in traffic emissions during the weekend (Jiménez et al., 2005). The decrease between summer and winter was also observed at MSY, where the T/B ratio was 3.58 ± 3.50 during summer compared to 2.44 ± 2.91 in winter due to the same phenomena. The lower values at MSY compared to BCN were a result of photochemical aging since toluene is scavenged more rapidly than benzene (Table 6) (Gelencsér et al., 1997; Seco et al., 2013) since MSY is located further from the sources of traffic and industry, which will most likely involve transported air masses and result in a lower T/B ratio.

Notably, anthropogenic emissions are generally higher during winter than summer at BCN, as observed for NO_2 and CO (Fig. 2) (in 't Veld et al., 2021; Pandolfi et al., 2016; Pérez et al., 2016; Querol et al., 2014; Querol et al., 2001; Viana et al., 2013) and previous studies of benzene and toluene at BCN (Filella and Peñuelas, 2006). Contrary to this, in our study, the mixing ratios of toluene and the C_8 aromatics in the atmosphere were higher during summer at BCN, while the winter levels were higher at MSY (Table 3). Currently, it remains unknown why this increase occurred during summer.

Factor 1 showed a high correlation with other anthropogenic contaminants in the study area, such as BC concentrations (summer: r = 0.73; winter: r = 0.83), NO_2 concentrations (summer: r = 0.46; winter: r = 0.66), and other anthropogenic factors, namely the *traffic & biomass burning factor* (*Factor 2)* (summer: r = 0.55; winter: r = 0.89) and the *isoprene oxidation factor* (*Factor 3*) (summer: r = 0.42; winter: r = 0.72), which will be discussed in their respective sections. Overall, *Factor 1* represents emissions from traffic and industry at BCN.

At MSY, the mixing ratios of *Factor 1* were considerably lower when compared to BCN due to its distance from anthropogenic sources. During summer, levels were negligible and increased in winter due to greater anthropogenic emissions. During summer at MSY, the *traffic & industry factor* showed some correlation with solar radiation (r = 0.42), with increasing concentrations during daylight hours when compared to the evening (Fig. 6), while the two peaks that coincided with rush hours at BCN were absent. All other correlations with anthropogenic contaminants were not statistically significant. This indicates that instead of an anthropogenic origin, the factor might have a minor biogenic contribution to MSY. This should be considered an option since toluene could be emitted by Mediterranean holm oaks and pines (Heiden et al., 2009; Holzinger et al., 2000; Misztal et al., 2015). Fig. S5 presents the diel variation of toluene and temperature for each day. Each diel variation shows a peak during midday on most measured days, which was absent for BCN. This correlation was only present for toluene and missing for the C_8 aromatics. Although the diel variation showed a similar pattern for both the toluene and the C_8 aromatics, the correlation between these two compounds at MSY was not as high (r = 0.52, compared to r = 0.94 at BCN for the same season). Both VOCs still had a significant correlation with other anthropogenic tracers (Fig. S3–4), which would indicate an

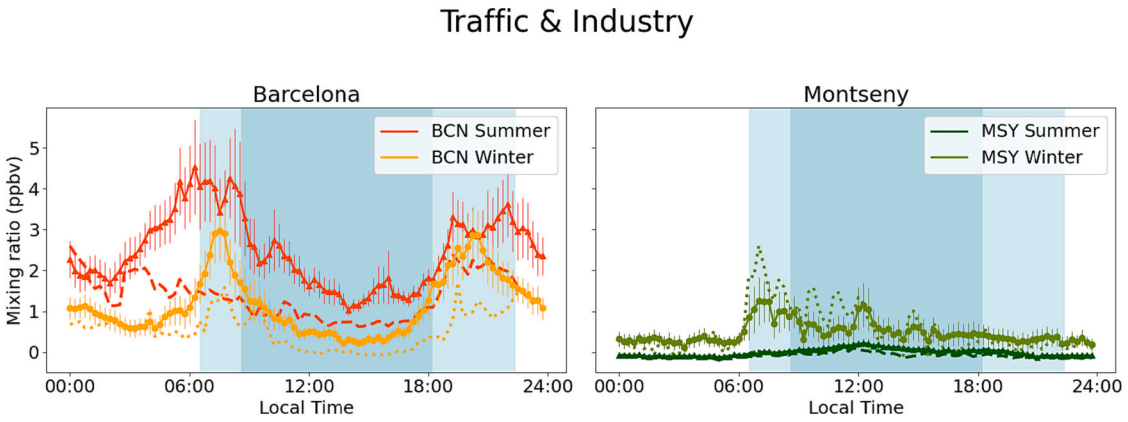

Fig. 5. Diel variation of 15-minute average concentrations of Factor 1 (Anthropogenic I: Traffic & Industry) at BCN (left) and MSY (right) over the entire week, with the respective standard deviations. Dotted lines represent weekends. Dark blue background represents daylight hours during winter, while blue background represents daylight hours during summer.

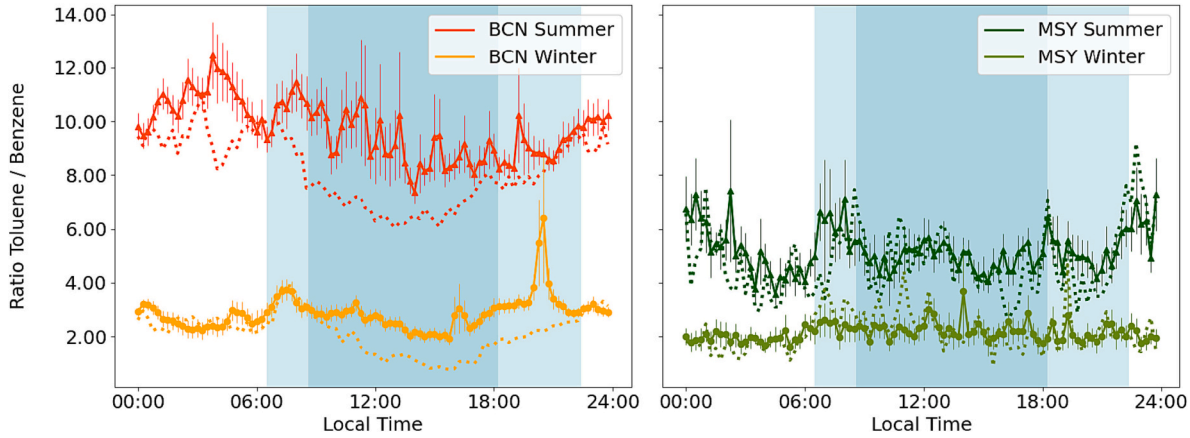

Fig. 6. Diel variation of the 15-minute average toluene to benzene (T/B) ratio in Barcelona (left) and Montseny (right), separated by season over the entire week. Dotted lines represent weekends. Dark blue background represents daylight hours during winter , while blue background represents daylight hours during summer.

anthropogenic origin for this factor with a minor biogenic contribution from toluene. Yáñez-Serrano et al. (2021a, b) identified a similar factor at a site located nearby the MSY station and attributed it to traffic emissions, which was the lowest contributing factor during summer, as we observed in our study. Tan et al. (2021) also found an anthropogenic source in Hong Kong with the same tracers, attributing it to industrial and traffic emissions.

3.2.2. *Factor 2: Anthropogenic II: Traffic & Biomass Burning*

Factor 2 was traced by benzene (69 %), acetaldehyde (67 %), and acetonitrile (36 %), as well as various oxidized VOCs (OVOCs), such as MEK (27 %), methanol (19 %), and C_8 aromatics (19 %). Both benzene and acetonitrile are typical markers of biomass burning, with studies also showing that acetaldehyde, MEK, and methanol can originate from biomass burning (Cerqueira et al., 2013; Holzinger et al., 1999; Li et al., 2014; Tan et al., 2021).

The mixing ratio of this factor was much higher during winter when compared to summer at both stations. While biomass burning can have various sources, such as forest fires and the burning of agricultural waste, the increase during winter indicated that this increase was due to residential heating, which was previously detected in the study area (Reche et al., 2012; Viana et al., 2013). The T/B ratio also confirmed this, with lower ratios during the winter season when compared to the summer at both stations, indicating a higher influence of biomass burning (Fig. 8).

Fig. 8 presents a scatterplot of the benzene and toluene mixing ratios. While they are mostly grouped together, showing a high T/B ratio, two periods deviated from this (marked in red). The first was at BCN on the 14th of February 2022 between 07:00 and 10:00 and the second was at MSY on the 13th of June 2022 between 17:00 and 21:30. During these events, the T/B ratio differentiated from the group to a ratio below 1, indicating biomass burning as the dominant source (Seco et al., 2013; Tan et al., 2021). However, the peaks coincided with increases in various other VOCs and pollutants; therefore, the origin of this factor cannot be completely attributed to biomass-burning events.

At BCN, *Factor 2* has a high correlation with the *traffic & industry* factor (*Factor 1*) (summer: $r = 0.80$; winter: $r = 0.87$) and BC concentrations (summer: $r = 0.82$; winter: $r = 0.79$), which indicates the anthropogenic origin of *Factor 2*. This is further confirmed by the two peaks in the morning and evening, as observed for the *traffic & industry factor* (*Factor 1*), which is common for anthropogenic contaminants at BCN. Notably, the levels of *Factor 2* were much higher during winter when compared to the summer period due to increased anthropogenic contamination, which can also be observed with the higher concentrations of the weekly averages when compared to weekends. During summer, this difference was also much smaller (Fig. 7).

Although biomass burning had a major impact on this factor at BCN, it is not likely its sole source. Benzene is emitted from traffic emissions, which cannot be ignored in an urban area such as BCN (Fernández-Iriarte et al., 2020; Gelencsér et al., 1997; Heeb et al., 2000). Furthermore, the diel variations of acetaldehyde and acetonitrile showed different patterns when compared to this factor (Fig. 3). Acetaldehyde can have various origins, such as fossil fuel combustion (Nogueira et al., 2015; Sinharoy et al., 2019; Xu et al., 2022), biomass burning (Cerqueira et al., 2013; Holzinger et al., 2005; Holzinger et al., 1999), hydrocarbon oxidation (Luecken et al., 2012), and even vegetation emissions (Seco et al., 2007). At BCN during winter, acetaldehyde showed the highest mixing ratios during midday, with an additional increase in the evening. However, there were no weekly patterns, with similar concentrations observed during weekly averages and weekend averages. The levels during summer were much lower, showing peaks in the morning and evening. The lower concentration during the day could be caused by the fact that acetaldehyde has an atmospheric lifetime of only a few hours (Possanzini et al., 2002; Seco et al., 2013) due to photochemical destruction (Atkinson and Arey, 2003), which resulted in lower mixing ratios being observed during the day in the summer season. This effect was not observed in the winter due to less sunlight and fewer daylight hours, which reduces the ability of acetaldehyde to be removed from the atmosphere when compared to summer (Filella and Peñuelas, 2006; Viskari et al., 2000).

Acetonitrile showed higher levels during the day when compared to the evening during both summer and winter at BCN, with higher levels in the winter (Fig. 3). Compared to acetaldehyde, the levels during weekends were much lower, indicating an anthropogenic source. Acetonitrile is generally considered a biomass burning marker with a minor source from fossil fuel combustion, which might be the main source at BCN (Holzinger et al., 2005; Holzinger et al., 1999). Given the stark difference between weekdays and weekends, this is most likely the case.

An investigation of the three biggest tracers of *Factor 2* indicates that while this factor partially included biomass burning at BCN, it also was likely a second traffic source in addition to *Factor 1*. Previous studies assessing sources of biomass burning at BCN stated that after the switch to natural gas, the contribution from residential heating in the particulate matter was relatively low (AIRUSE, 2016; Amato et al., 2016; Viana et al., 2013). Notably, its contribution remains significant since a study conducted during winter 2011 at BCN attributed 8 % of the $PM_{2.5}$ mass to biomass burning (Reche et al., 2012).

At MSY, the peaks associated with anthropogenic traffic emissions were absent due to the distance from their source, with the mixing ratios of this factor being mostly even throughout the day. During summer, the diel variation of *Factor 2* showed a peak at approximately 18:00. (Fig. 7);

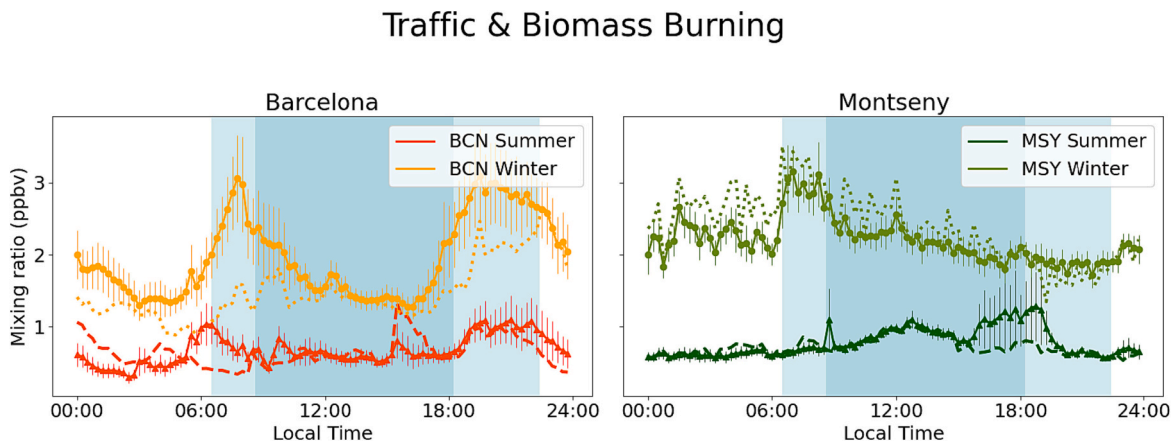

Fig. 7. Diel variation of 15-minute average concentrations of Factor 2 (Anthropogenic II: Traffic & Biomass burning) at BCN (left) and MSY (right) over the entire week, with the respective standard deviations. Dotted lines represent weekends. Dark blue background represents the daylight hours during winter, while blue background represents the daylight hours during summer.

however, this was due to a biomass-burning event observed on the 13th of June. The correlation with BC further indicates that this peak was caused by a biomass burning event, with a correlation of $r = 0.66$ for the entire dataset of *Factor 2* during summer, while the *traffic & industry factor* (*Factor 1*) did not correlate with either this factor or the BC levels. In winter, this factor likely incorporated pollutants from residential heating and other sources transported from BCN and surrounding industrial areas. This was also confirmed by a correlation with the *traffic & industry factor* ($r = 0.65$), as well as the appearance of a peak at 07:00 for all tracers of *Factor 2*.

The diel variation of benzene at MSY showed similar patterns to the *traffic & biomass factor* (*Factor 2*); however, just like BCN, acetaldehyde and acetonitrile had different diel variations when compared to *Factor 2*. Both compounds showed higher levels in summer than in winter, increasing during the day and declining in the afternoon. In the case of acetonitrile, this could include long-range transport from forest fires in the Mediterranean area (Seco et al., 2013). Notably, acetonitrile levels were significantly lower when compared to BCN, suggesting that acetonitrile at BCN was of local origin.

Acetaldehyde also has a biogenic origin, which was more prominent at MSY (Lewis et al., 2005; Luecken et al., 2012; Possanzini et al., 2002). Furthermore, it can also be formed in the atmosphere by photochemical production from akenes (including biogenic alkenes such as terpenes) (Luecken et al., 2012; Seco et al., 2007). Higher levels in the summer compared to winter could be a result of the increased physiological activity of vegetation and increased secondary production due to greater photochemical activity, as well as higher local acetaldehyde emissions from forest fires (Seco et al., 2011).

A previous study by Yáñez-Serrano et al. (2021a) near MSY did not identify a biomass burning source during summer due to its low contributions from biomass burning during this season and the lack of confirmed wildfires during their study. Tan et al. (2021) also identified a biomass burning source in Hong Kong using the same tracers as this study.

3.2.3. Factor 3: isoprene oxidation source

Factor 3 was traced by isoprene (81 %) and MVK + MACR (65 %), both of which are oxidation products of isoprene (Ling et al., 2019; Liu et al., 2013). This factor also had lower levels of OVOCs attributed to it, such as MEK (15 %), acetone (10 %), and monoterpenes (10 %). The diel variations of MSY showed a clear increase during daylight in summer, which was less pronounced at BCN (Fig. 9). Both stations confirmed this trend with a significant correlation of *Factor 3* with solar radiation (BCN: $r = 0.48$; MSY: $r = 0.52$) at both stations (Figs. S1 and S3).

At MSY, the diel variation indicated a biogenic origin for isoprene (Fig. 3), which is known to be emitted by vegetation (Pacifico et al., 2011; Sanadze, 2004). This was further confirmed by the high correlation between this factor and the *monoterpene factor* (*Factor 4*) ($r = 0.91$) during summer, which was also emitted by biogenic activity (see description for Factor 4). This confirms the findings of Yáñez-Serrano et al. (2021a), who also measured high levels of isoprene and its oxidation products in Montseny Natural Park (a few kilometers from our station) during summertime and found a diel variation similar to the solar radiation cycle, which was also observed in this study (r = 0.52). This could be surprising since the forest at MSY is dominated by holm oak, which typically emits isoprene at a lower rate (only 5 % compared to monoterpenes) (Peñuelas et al., 2009). Furthermore, several *Quercus* species, such as *Quercus ilex* (a dominant species in the MSY region), also emit isoprene (Fernández-Martínez et al., 2018). However, a previous report for the same MSY site by Seco et al. (2011) found summertime isoprene mixing ratios amounting to approximately two-thirds of those of monoterpenes and with very similar diel patterns, which is in agreement with the present study and suggests that other vegetation present in those forests and the surrounding areas are isoprene emitters. While the exact origin of isoprene cannot be confirmed yet, it was speculated these come from *Erica arborea*, a shrub located near MSY and known to emit a considerable amount of isoprene (Pagès et al., 2020; Yáñez-Serrano et al., 2021a). Yáñez-Serrano et al. (2021a) also hypothesized that isoprene could originate from local vehicle exhaust emissions (Borbon et al., 2001), but no correlation was found between isoprene and any anthropogenic contaminant (Fig. S3). Meanwhile, concentrations during winter were considerably lower due to the smaller biogenic emissions as a result of reduced solar radiation and temperature. Moreover, the diel pattern of the isoprene to MVK + MACR ratio (Fig. 10) showed that during summer at MSY, the ratios decrease during daylight hours until 18:00, with a maximum at approximately 09:00. This indicates that biogenic isoprene becomes oxidized into secondary MVK and MACR.

At BCN, a different situation occurred. *Factor 3* showed an increase during daylight hours and decreased in the afternoon, with an additional small peak in the morning and evening (Fig. 9). The morning and evening peaks coincide with those from other anthropogenic emissions, which implies there was also an anthropogenic source for this factor (Fig. 2). The anthropogenic origin was further confirmed with the positive correlation with BC ($r = 0.50$), the *traffic & biomass burning factor* (*Factor 2*) ($r = 0.56$), and the *traffic & industries factor* (*Factor 1*) ($r = 0.44$) (Fig. S1) during summer. The correlation was even higher during winter, with a positive correlation with BC ($r = 0.46$), *traffic & biomass burning factor* (*Factor 2*) ($r = 0.72$), and the *traffic & industries factor* (*Factor 1*) ($r = 0.60$). Isoprene is known to be emitted by anthropogenic

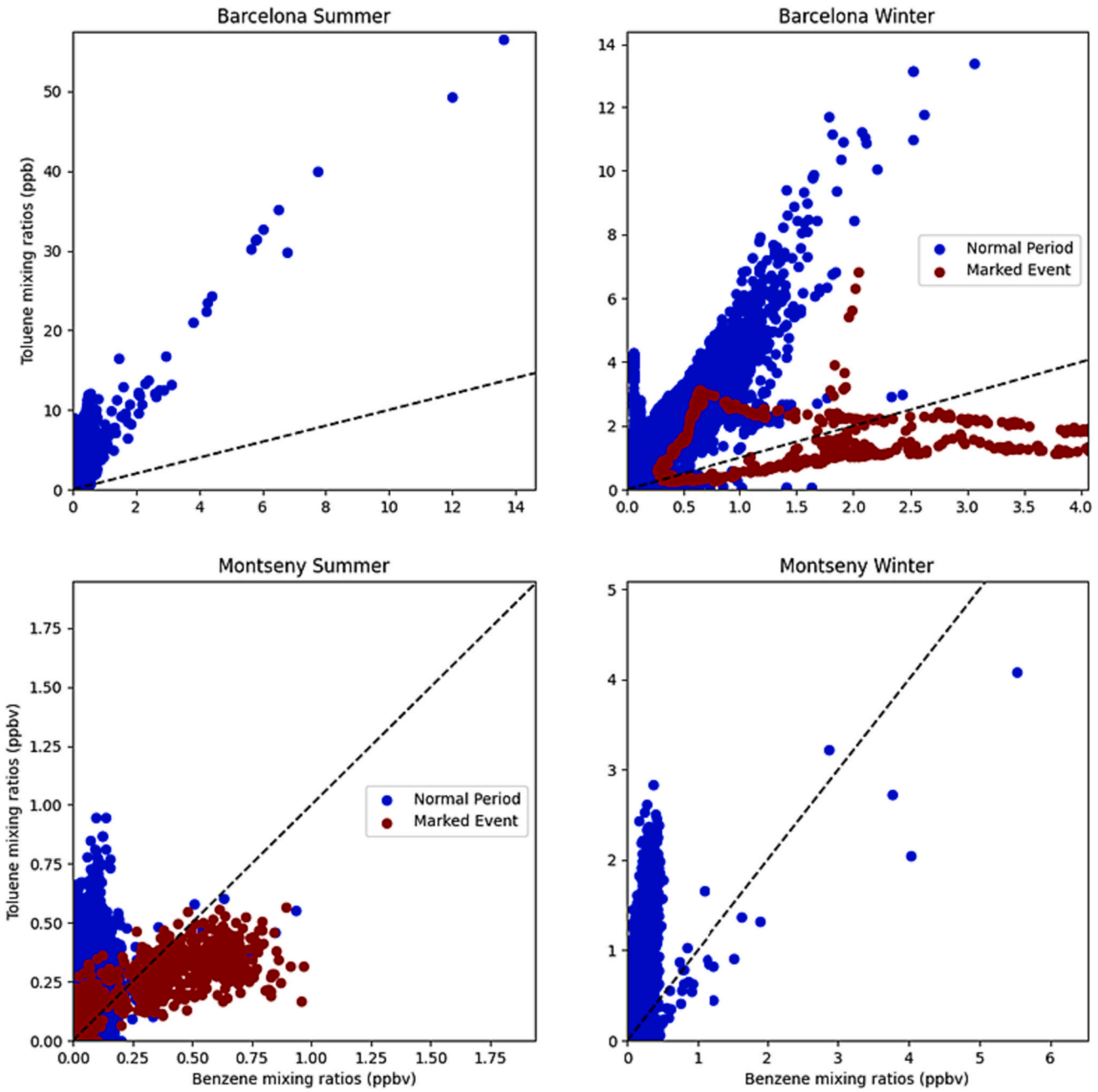

Fig. 8. Scatter plot between benzene concentrations (x-axis) and toluene concentrations (y-axis) for the four measurement periods. Red points indicate a period that differentiates from the norm. Dotted black lines indicate the 1:1 ratio between toluene and benzene.

activities, particularly traffic (Borbon et al., 2002, Borbon et al., 2001; Filella and Peñuelas, 2006; Wagner and Kuttler, 2014; Yee et al., 2020). However, other anthropogenic VOCs can also contribute to the signal of *m/z* 69 since it is a common fragment of cycloalkenes (Gueneron et al., 2015). Nevertheless, the maximum isoprene mixing ratios in summer occurred at 13:00, when temperature and solar radiation were also at their maximum. This observation suggests that a biogenic source remains present at BCN, which is logical given the forests surrounding the area.

The isoprene oxidation factor was previously identified by Yáñez-Serrano et al. (2021a) in Montseny as a biogenic source along with monoterpenes. While monoterpenes are mostly of biogenic origin, isoprene is not necessarily biogenic. Combining the datasets of the two stations (i.e., BCN and MSY) separated this biogenic source between the *isoprene oxidation factor* (*Factor 4*) and the *monoterpene factor* (*Factor 5*). The *isoprene oxidation factor* is mostly biogenic at MSY, with high levels in the summer and a clear correlation with temperature (Fig. S3). Meanwhile, at BCN, an additional anthropogenic source of isoprene exists, especially during winter, as shown by the diel variation and correlation with other anthropogenic contaminants (Fig. 10; Fig. S1).

3.2.4. Factor 4: monoterpenes

The monoterpene factor (Factor 4) was mostly traced by monoterpenes (84 %), with minor contributions from methanol (10 %) and C_8 aromatics (10 %). The monoterpene factor was emitted from biogenic sources at MSY, as seen in the diel pattern (Fig. 11). Just like for the isoprene oxidation factor, levels were extremely high during the day while being low at night and in the evening. Furthermore, a clear distinction between seasons is apparent since this factor exhibited its minimum mixing ratios during winter without any diel variation,

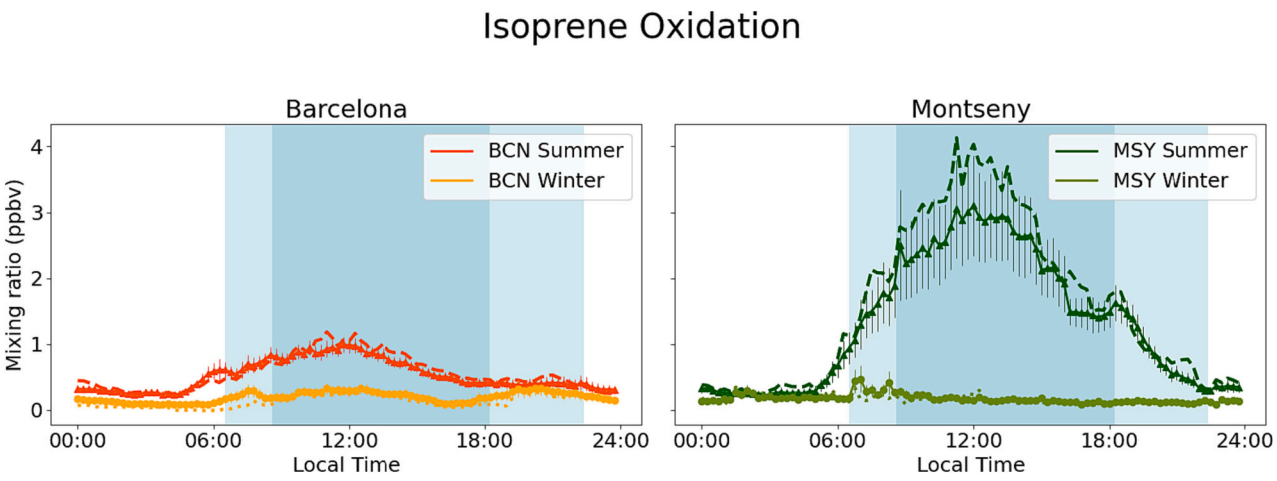

Fig. 9. Diel variation of 15-minute average concentrations of Factor 3 (isoprene oxidation source) at BCN (left) and MSY (right) over the entire week, with the respective standard deviations. Dotted lines represent weekends. Dark blue background represents the daylight hours during winter, while blue background represents the daylight hours during summer.

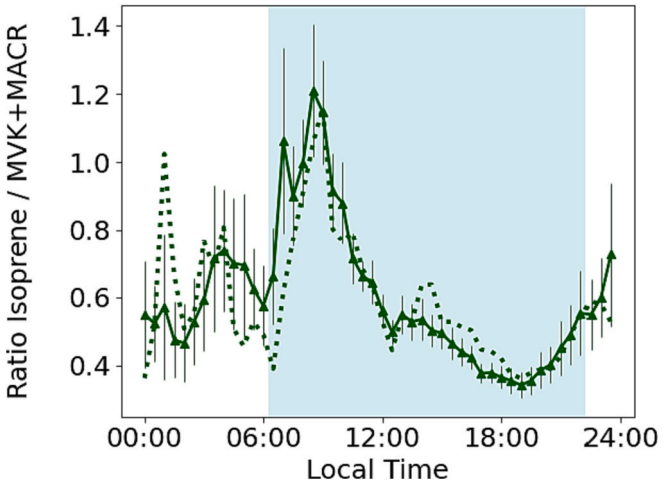

Fig. 10. Diel variation of the ratio of isoprene to MVK + MACR at MSY during summer. Dotted lines represent weekends, and the blue background represents the daylight hours.

whereas it had a clear diel variation correlating with sunlight and temperature in summer (Fig. S3–4). The high levels measured are due to the MSY station being embedded among holm oak trees, which emit these compounds in relevant quantities (Peñuelas et al., 2009; Seco et al., 2013, Seco et al., 2011). This factor was previously identified by Yáñez-Serrano et al. (2021a) at Montseny, where it was combined with the isoprene oxidation factor into a single biogenic source.

This was not the case for BCN, where the diel variation did not resemble one increasing with sunlight. This factor did correlate with the anthropogenic factors (*traffic & biomass burning and traffic & industries*) during both seasons, with a correlation factor between 0.61 and 0.72 during summer and 0.71 and 0.78 during winter (Fig. S1–2). However, the peaks in the morning and evening did not coincide with the peaks of the anthropogenic contaminants (Figs. 2 and 10). Hellén et al. (2012) proposed a traffic-related origin of monoterpenes since the diel variation of monoterpenes resembles those of anthropogenic aromatics; however, as previously mentioned, the peaks at BCN do not coincide with said anthropogenic aromatics. It is more likely that the diel variation shape was caused by the rapid reaction of monoterpenes with daytime generated $OH^{\bullet}$ radicals and dilution by atmospheric mixing, as was reported previously in the study area (Filella and Peñuelas, 2006; Harrison et al., 2001). Although lower levels were observed during weekends, those values might still indicate an anthropogenic origin. The reaction rates with $OH^{\bullet}$, presented in Table 6, indicate that the reactivity of

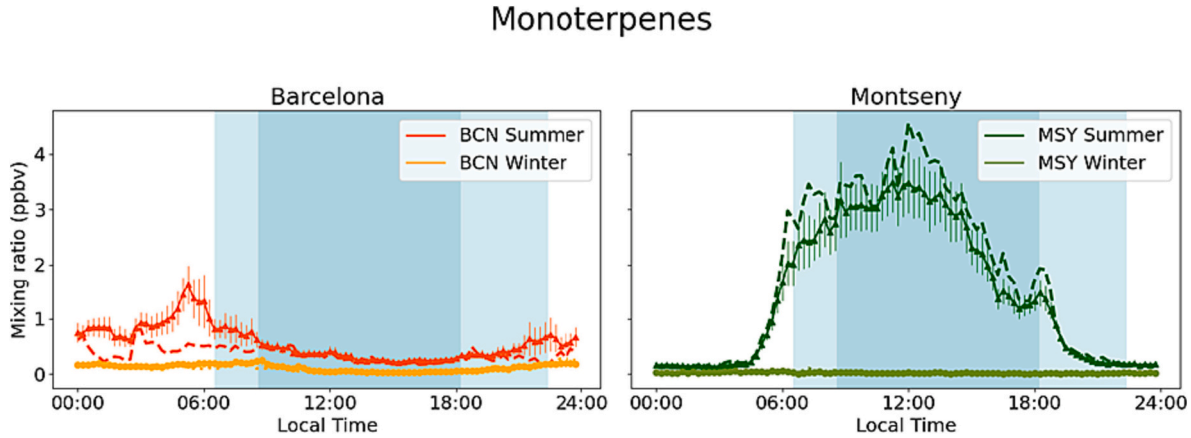

Fig. 11. Diel variation of 15-minute average concentrations of Factor 4 (Monoterpenes) at BCN (left) and MSY (right) over the entire week, with the respective standard deviations. Dotted lines represent weekends. Dotted lines represent weekends. Dark blue background represents the daylight hours during winter, while blue background represents the daylight hours during summer.

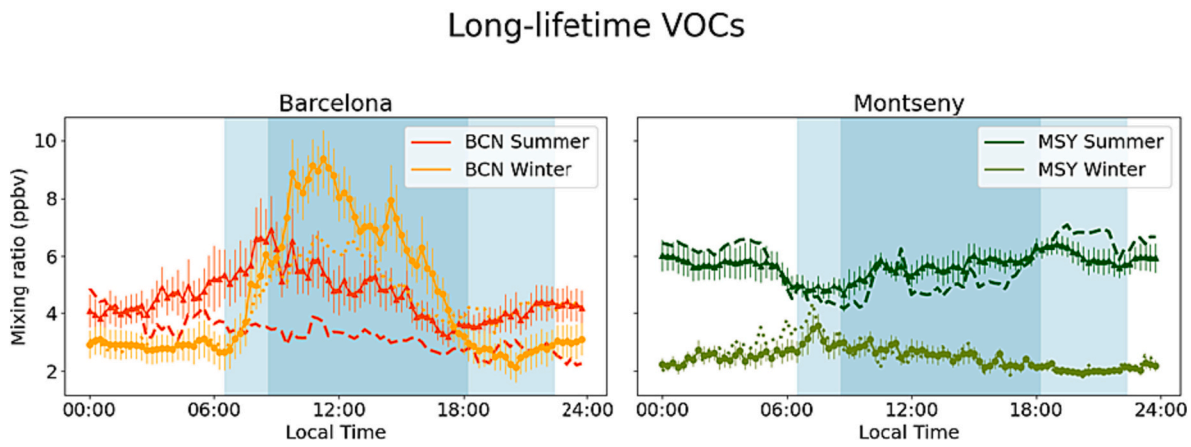

Fig. 12. Diel variation of 15-minute average concentrations of Factor 5 (Long-lifetime VOCs) at BCN (left) and MSY (right) over the entire week, with the respective standard deviations. Dotted lines represent weekends. Dotted lines represent weekends. Dark blue background represents the daylight hours during winter, while blue background represents the daylight hours during summer.

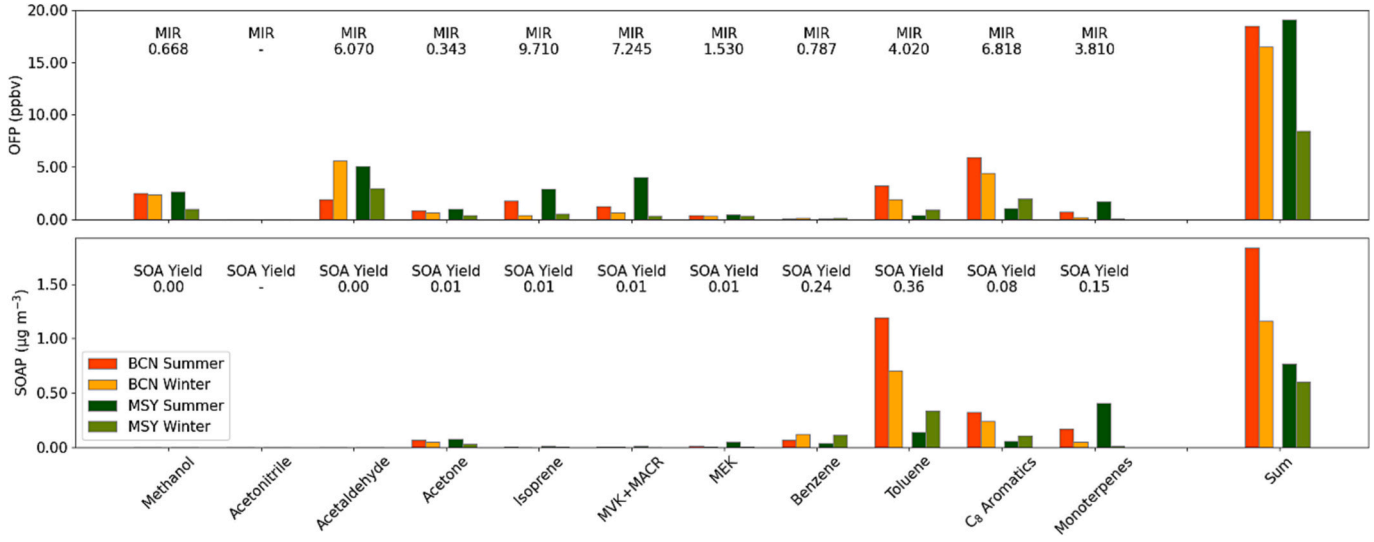

Fig. 13. Summary of the OFP (top) and SOAP (bottom) at BCN and MSY. OFP are expressed in ppbv, and SOAP in μg m^{-3}.

monoterpenes is at least 10- to 100-fold faster when compared to the other VOCs.

3.2.5. *Factor 5: long-lifetime VOCs*

The final factor was a mixture of the remaining VOCs in the study area. These were traced by various OVOCs, including acetone (71 %), methanol (69 %), acetonitrile (61 %), MEK (40 %), MVK + MACR (31 %), and acetaldehyde (23 %).

Methanol and acetone had the highest mixing ratios at both stations during both seasons, which can be attributed to their long lifetime in the atmosphere and the fact that they are formed from the oxidation of other VOCs (Seco et al., 2007) (Table 6). This resulted in high background levels, as observed in previous studies (Filella and Peñuelas, 2006; Lewis et al., 2005; Seco et al., 2013; Yáñez-Serrano et al., 2021a). Acetonitrile had much lower mixing ratios but also has a long atmospheric lifetime ranging from months to years (Sanhueza et al., 2004). Therefore, this factor was called the *long-lifetime VOCs factor*.

At BCN, the *long-lifetime VOCs factor* showed a similar diel pattern to those of methanol and acetone, which was similar to other anthropogenic contaminants during summertime (Fig. 12). This resulted in positive correlations with said factors (*traffic & industries*: 0.49; *traffic & biomass burning*: 0.52), as well as the observation of two peaks—one early in the morning and one in the evening—with much lower mixing ratios during weekends. At BCN, Filella and Peñuelas (2006) (and references therein) found that both methanol and acetone were emitted by road traffic, which resulted in peaks during rush hours. The observed decrease of *factor 5* during the day would be a result of photochemical destruction and dilution effects. The anthropogenic origin of these VOCs is further confirmed by the lower mixing ratios over weekends.

During winter at BCN, the highest mixing ratios of *Factor 5* occurred at midday, with a small peak in the evening (Fig. 12). During summer, the disparity between the weekday and weekend averages was highly accentuated (Fig. 12); however, this difference was only observed in the middle of the day during winter. This suggests that at BCN, this factor has a combination of sources—mostly anthropogenic and from atmospheric oxidation—and that this combination can change with the season. The exact reason for the higher levels could not be determined but is hypothesized to be a combination of increased anthropogenic emissions, diminished photochemical destruction of methanol and acetone due to less sunlight, and a more stable weather condition.

During summer at MSY, the long-lifetime VOCs factor mixing ratio does not represent the trends of any VOCs. This is most likely a result of the different trends that all the VOCs have at this station, which averages to an overall neutral trend. Methanol showed three peaks (Fig. 3), with

one in the morning (08:00) possibly coinciding with stomatal opening (Fall and Benson, 1996; Hüve et al., 2007), and two more around midday and in the evening. This suggests both the biogenic and photo-oxidation origins of methanol at the MSY station. On the other hand, acetone only displayed a peak during the day that was highly correlated with temperature ($r = 0.75$) and the biogenic sources (isoprene oxidation: $r = 0.69$; monoterpenes $r = 0.56$). This would indicate that, like methanol, acetone at MSY can be both formed due to photo-oxidation and biogenic emissions at MSY. The only difference was that acetone did not have a stomatal release in the morning, hence the lack of a morning peak.

On the other hand, during the winter season, all three long-lifetime VOCs showed no diel variation due to lower biogenic emissions and sunlight. This indicates that they are mostly long-range transported VOCs due to their lengthy atmospheric lifetimes.

3.3. Ozone formation potential

The contribution of VOCs to the formation of O_3 was estimated using the MIR method to calculate and assess the contribution of each VOC to ozone formation. Table 5 presents the MIR of each VOC. All MIRs were obtained from Venecek et al. (2018), except for acetonitrile, which has a currently unknown MIR. However, it is important to consider that the MIR values used in this comparison are based on an urban environment, which limits the accuracy of the estimated OFP for MSY (Venecek et al., 2018), although the MIR has been applied in rural environments to estimate the OFP (Gómez et al., 2020; Kumar et al., 2018; Luo et al., 2020). The results of the OFP are presented in Table 5 and Fig. 13. The presented OFP is based on the observed mixing rations of VOCs. The author notes that the actual OFP should be higher due to the photochemical loss of VOCs (Liu et al., 2023; Wu et al., 2023). The OFP of the sum of the VOCs was similar during summer at both stations, with 18.51 ppbv at BCN and 19.07 ppbv at MSY. During winter, a clear difference was observed. The winter OFP was 16.50 ppbv at BCN, only slightly lower compared to the summer season, while the OFP was considerably lower at MSY during winter at 8.42 ppbv. The differences in OFP between the stations and seasons were due to low concentrations of high-MIR VOCs during winter in the rural area. There are two groups with high MIR values among our measured VOCs. These were primarily the aromatics, which are mostly anthropogenic and thus quite low at MSY, with the second-largest group being biogenic VOCs such as isoprene, its oxidation products, and monoterpenes, whose emissions considerably decrease during winter due to a decrease in sunlight. The OFP does not completely account for the O_3 concentrations measured simultaneously. At BCN during winter, the OFP was 36 % of the total O_3, while it was 13 % at MSY during winter. Meanwhile, during summer, BCN exhibited 28 % of the total O_3, while MSY exhibited 22 %. This dispersion can be due to the limited VOC set measured, as well as various other sources of O_3.

Table 5
Maximum incremental reactivity (MIR) and whole-campaign average ozone formation potential (OFP) of the measured VOCs for the different seasons at both stations. The MIR shown for MVK + MACR and C_8 aromatics are averages of the MIR of all compounds included in those categories. Acetonitrile has currently an unknown MIR and was therefore left blank.

VOC	Type	MIR (g O_3/g VOC)	OFP (ppbv)			
			BCN		MSY	
			Winter	Summer	Winter	Summer
Methanol	OVOC	0.67	2.34 ± 3.26	2.49 ± 2.39	0.98 ± 0.54	2.60 ± 1.12
Acetonitrile	OVOC	–	–	–	–	–
Acetaldehyde	OVOC	6.07	5.60 ± 5.25	1.89 ± 1.64	2.94 ± 1.73	5.07 ± 2.69
Acetone	OVOC	0.34	0.66 ± 0.65	0.86 ± 0.73	0.35 ± 0.17	0.95 ± 0.36
Isoprene	HVOC	9.71	0.35 ± 1.57	1.79 ± 1.52	0.52 ± 0.83	2.90 ± 4.03
MVK + MACR	OVOC	7.25	0.62 ± 0.53	1.21 ± 1.09	0.33 ± 0.46	3.98 ± 3.61
MEK	OVOC	1.53	0.34 ± 0.28	0.36 ± 0.32	0.29 ± 0.25	0.46 ± 0.28
Benzene	HVOC	0.79	0.11 ± 0.16	0.07 ± 0.09	0.11 ± 0.07	0.03 ± 0.04
Toluene	HVOC	4.02	1.89 ± 2.66	3.22 ± 4.01	0.90 ± 1.26	0.36 ± 0.40
C_8 aromatics	HVOC	6.82	4.39 ± 6.96	5.91 ± 6.87	1.95 ± 2.62	1.01 ± 1.02
Monoterpenes	HVOC	3.81	0.19 ± 0.27	0.71 ± 0.94	0.06 ± 0.08	1.71 ± 2.02
Sum			*16.50 ± 16.19*	*18.51 ± 16.46*	*8.42 ± 6.03*	*19.07 ± 12.62*

Comparing the hydrocarbon VOCs (HVOCs) and OVOCs showed a similar situation during winter at both stations, where OVOCs drove the OFP slightly higher, with 7.22 ppbv (51 %) at BCN and 4.89 ppbv (58 %) at MSY, compared to 6.93 ppbv (49 %) and 3.54 (42 %) for HVOC at BCN and MSY, respectively. The situation was quite different during the summer months for the two stations. At BCN, the OFP was mostly driven by HVOCs, with 11.7 ppbv (63 %) compared to 6.81 ppbv (37 %) of OVOCs. At MSY, the situation was reversed, where the OFP was primarily driven by OVOCs, with 13.06 ppbv (68 %) compared to 6.01 ppbv (32 %) of HVOCs. This difference in contribution is a commonly observed phenomenon, where OVOCs contribute significantly more to rural areas when compared to urban areas (Chen et al., 2022; Louie et al., 2013; Luo et al., 2011).

At BCN, the OFP primarily originates from the *traffic & industry factor* (*Factor 1*) since both toluene and C_8 aromatics, which were the main tracers of this factor, together made up 50 % of the estimated OFP during summer, with 9.13 ppbv. On the other hand, due to the relatively lower MIR and mixing ratios of benzene, it contributed very little toward OFP. The total OFP from the aromatics (benzene, toluene, and C_8 aromatics) was nearly 1.5 times lower during winter (6.28 ppbv) due to the lower mixing ratios of toluene and C_8 aromatics, accounting only for 39 % of the total OFP. At MSY, the contribution of the *traffic & industries factor* was significantly lower, with the relative contribution of toluene and C_8 aromatics to OFP being 35 % (2.85 ppbv) during winter, which is nearly 2.2-fold lower when compared to BCN during the same season. During summer, the contribution of these aromatics to OFP was only 7 % with 1.37 ppbv, representing one of the smallest contributing sources and 6.6 times lower when compared to summer at BCN. Although this is worth keeping in mind, since MSY is a rural area, most toluene and C_8 aromatics will be transported from industrial and urban sources and are thus already photo oxidized to O_3 and SOAs when the air masses reach the station (Seco et al., 2013).

The biogenic sources, which are the *monoterpenes factor* (*Factor 4*) and the *isoprene oxidation products* (*Factor 3*), had much higher mixing ratios during summer due to increased biogenic emissions at both stations. The combination of isoprene, MVK + MACR, and monoterpenes accounted for 20 % of the OFP during summer at BCN. This significantly decreased during winter to a combined 7 %, with an OFP of 1.16 ppbv compared to 3.71 ppbv during summer. Notably, most of the OFP during winter originated from isoprene and its oxidation products since the monoterpene's contribution at BCN was low. As previously established, this also includes anthropogenic isoprene. At MSY, these sources were mainly biogenic and contributed much more to the total OFP. During summer, the biogenic sources made up 45 % of the total OFP with 8.59 ppbv, which was much lower during winter when they only comprised 11 % of the total OFP with 0.91 ppbv. This made biogenic VOCs the main driver of OFP at MSY during summer.

The final significant contribution to OFP was from acetaldehyde, which, with its high MIR and mixing ratios, contributed significantly to the OFP at both stations. During winter, it contributed 34 % of the total OFP at BCN with 5.60 ppbv, which was much higher than during summer, when it only contributed 10 % of the total OFP with 1.89 ppbv.

During winter at MSY, acetaldehyde also contributed 35 % of the total OFP, with 2.94 ppbv, while during summer it only contributed 27 % of the total OFP but it contributed more (5.07 ppbv) in absolute terms. Ultimately, acetaldehyde contributed relatively the most during the winter season at both stations, even though the actual OFP was higher during the summer season at MSY. Methanol followed closely with 12 to 14 % of the total OFP at all stations.

It must be noted that the OFP for isoprene, monoterpenes, and the aromatic VOCs are underestimated in this study. Previous studies have reported that these VOCs can have an underestimation between 50 and 90 % of the observed mixing ratios due to photochemical loss (Gu et al., 2023; Liu et al., 2023; Stroud et al., 2001; Wu et al., 2023; Yang et al., 2022). Since these compounds have a relatively high MIR, the impact of the underestimation of the OFP is even greater and should be considered. This is especially true for the *isoprene oxidation products* as isoprene and MVK + MACR have the highest MIRs of the measured VOCs, closely followed by toluene and C_8 aromatics of the *traffic & industry* source.

3.4. SOA formation potential

Most of the existing literature has estimated the SOAP using the relative SOAP to toluene ratio obtained from Derwent et al. (2010). While useful, the list presented there does exclude some essential VOCs that we measured in our study. Therefore, we obtained the SOAP from Gu et al. (2021), who reported the SOA yield of various VOCs included in this study. It is crucial to state that this method, like the OFP, has the limitation that the SOA yield was calculated based on an urban environment with a high NO_x atmosphere, which influences SOA formation (Camredon et al., 2007). While this situation applies to BCN, it is more inaccurate in the case of MSY. Additionally, it is worth mentioning that the SOA yields used $OH^\bullet$ as the primary oxidant to form SOA (Gu et al., 2021). O_3 is a secondary oxidant that can also form SOA, and with O_3 levels being generally higher in the MSY rural area, its capability to oxidize will increase accordingly. However, the reaction rates of VOCs with O_3 are 10^5 to 10^{11} times lower (Atkinson and Arey, 2003; Atkinson and Carter, 1984) than those with $OH^\bullet$, thereby diminishing the impact of this difference. The results of the SOAP are presented in Table 7 and Fig. 13. Finally, the presented SOAP is based on the observed mixing rations of VOCs. The authors note that the actual SOAP should be higher due to the photochemical loss of VOCs (Liu et al., 2023; Wu et al., 2023).

Overall, aromatics contributed the most due to their high SOA yields at both stations during both seasons (Table 7, Fig. 13). Since the mixing ratios of these aromatic compounds were much higher at BCN, a much higher SOAP was observed in this study. Due to the aromatic VOCs' high SOA yields, they contributed the most to the SOAP at both stations during both seasons (Table 7). Since the mixing ratios of these aromatic compounds were much higher at BCN, the SOAP was considerably higher compared to MSY. At MSY, the SOAP was similar between the two seasons but was dominated by anthropogenic aromatic compounds (benzene, toluene, C_8 aromatics) during winter, while the monoterpenes were a considerable source of SOAP in summer.

This would indicate that *traffic & industry* (*Factor 1*) was the main contributor to SOA formation from the measured VOCs at BCN since none of the remaining OVOCs and isoprene oxidation products have a significant SOA yield. Although monoterpenes have a significant SOA yield, the levels at BCN were much lower, resulting in minimal influence. However, the diel variation of the *monoterpene factor* (*Factor 4*) suggests that during summer at BCN, monoterpenes were rapidly reacting with daytime- generated $OH^\bullet$ radicals, which would result in the formation of both O_3 and SOA; therefore, the actual contribution of monoterpenes would be much higher than the values given in Table 7.

At MSY during winter, the *traffic & industry* factor (*Factor 1*) seemed to be the greatest source of SOA in the area. However, as was the case with the OFP, the actual SOAP might be higher as the transported toluene and C_8 aromatics deplete during transport. During summer, the monoterpenes were the main contributors to the SOAP, while other biogenic compounds, such as isoprene, did not contribute as much due to their low SOA yields.

It must be noted that the SOAP for isoprene, monoterpenes, and the aromatic VOCs are underestimated in this study. Previous studies have reported that these VOCs can have an underestimation between 50 and 90 % of the observed mixing ratios due to photochemical loss (Gu et al., 2023; Liu et al., 2023; Stroud et al., 2001; Wu et al., 2023; Yang et al., 2022). Since these compounds have a relatively high SOA Yield, the impact of the underestimation of the SOAP is even greater and should be considered. This is especially true for the *traffic & industry* source toluene and C_8 aromatics have the highest SOA yields of the reported VOCs, closely followed by the monoterpenes. For the SOA yield the underestimation of isoprene is less of an issue due to its low reported SOA yield.

4. Conclusions

The study presents the first urban VOC source apportionment in Spain, and also shows the possibility of using a multisite VOC PMF to use as an comparison between an urban background station and rural background station to determine the most significant contributors to O_3 and SOA formation. In this study, we quantified 11 VOC mixing ratios during summer and winter at both the BCN urban background site and the MSY rural background site (Table 5). Applying PMF to the combined dataset revealed five factors (Table 6). The first factor, *traffic & industries* (*Factor 1*), originated from anthropogenic sources such as traffic and industry in and around Barcelona, mostly consisting of aged air masses at MSY. The second factor, *traffic & biomass burning* (*Factor 2*), represented a secondary source combining traffic emissions and biomass burning. The third factor, *isoprene oxidation* (*Factor 3*), was associated with isoprene and its oxidation products, which had both anthropogenic and biogenic origins at BCN and were mostly biogenic at MSY. The fourth factor, *monoterpenes* (*Factor 4*), was predominantly biogenic at both stations, with lower levels at BCN due to rapid oxidation by $OH^\bullet$ and lower biogenic emissions in the area. The fifth factor (*Factor 5*) represented a mixture of VOCs with longer atmospheric lifetimes and included methanol, acetone, and acetonitrile, which had longer lifetimes when compared to other VOCs.

At BCN, the results demonstrated that both O_3 and SOA formation were predominantly driven by anthropogenic emissions, particularly those originating from the *traffic & industries factor* (38 and 49 % of the OFP during winter and summer, respectively). The aromatic compounds had a significant impact on the OFP and SOAP due to their high MIR and SOA yields (Tables 5 & 7). Both the OFP and SOAP showed seasonality with higher levels during the summer, primarily due to the higher levels of observed toluene and C_8 aromatic mixing ratios during summer. The MSY rural background site exhibited a different pattern, where both OFP and SOAP were driven by aged anthropogenic emissions, predominantly

Table 6
Reactivity of the listed VOCs in $cm^3 molecules^{-1}\ s^{-1}$ for three different oxidants: $OH^\bullet$, O_3, and NO_3. Values obtained from (Atkinson and Arey (2003). Values with * obtained from (Atkinson and Carter (1984). K-rates of acetonitrile and MEK were not reported in the found sources.

VOC	k-rate $OH^\bullet$	k-rate O_3	k-rate $NO_3^\bullet$
	$cm^3 molecule^{-1}\ s^{-1}$		
Methanol	0.94×10^{-12}	–	1.3×10^{-16}
Acetonitrile	–	–	–
Acetaldehyde	1.50×10^{-11}	2.00×10^{-20} *	2.7×10^{-15}
Acetone	0.17×10^{-12}	–	$< 3 \times 10^{-17}$
Isoprene	1.00×10^{-10}	1.27×10^{-17}	7.0×10^{-13}
MVK + MACR	2.45×10^{-11}	0.32×10^{-17}	2×10^{-15}
MEK	–	–	–
Benzene	1.22×10^{-12}	7.00×10^{-23} *	$< 3 \times 10^{-17}$
Toluene	5.63×10^{-12}	6.08×10^{-23} *	7×10^{-16}
C_8 aromatics	1.45×10^{-11}	1.03×10^{-19} *	4.43×10^{-16}
Monoterpenes	1.55×10^{-10}	1.87×10^{-15}	2.67×10^{-11}

Table 7
SOA yield and whole-campaign average SOA formation potential (SOAP) in μgm^{-3} of the measured VOCs for the different seasons at both stations (Gu et al., 2021). The SOA yield shown for MVK + MACR and C_8 aromatics are averages of the SOA yield of all compounds included in those categories. The SOA yield of acetonitrile is not reported and is therefore missing.

VOC	SOA Yield	SOAP (μgm^{-3})			
		BCN		MSY	
		Winter	Summer	Winter	Summer
Methanol	0	0	0	0	0
Acetonitrile	–	–	–	–	–
Acetaldehyde	0	0	0	0	0
Acetone	0.01	0.051 ± 0.050	0.066 ± 0.056	0.027 ± 0.013	0.073 ± 0.027
Isoprene	0.01	0.001 ± 0.005	0.006 ± 0.005	0.002 ± 0.003	0.009 ± 0.013
MVK + MACR	0.01	0.001 ± 0.001	0.003 ± 0.002	0.001 ± 0.001	0.009 ± 0.008
MEK	0.01	0.007 ± 0.006	0.008 ± 0.007	0.006 ± 0.005	0.049 ± 0.030
Benzene	0.24	0.119 ± 0.171	0.071 ± 0.094	0.114 ± 0.071	0.033 ± 0.047
Toluene	0.36	0.700 ± 0.988	1.192 ± 1.487	0.334 ± 0.468	0.135 ± 0.147
C_8 aromatics	0.08	0.238 ± 0.377	0.320 ± 0.372	0.105 ± 0.142	0.054 ± 0.055
Monoterpenes	0.15	0.046 ± 0.063	0.168 ± 0.225	0.014 ± 0.019	0.404 ± 0.478
Sum		*1.163 ± 1.535*	*1.833 ± 2.063*	*0.603 ± 0.633*	*0.766 ± 0.627*

from the *traffic & industries factor*, during winter. In contrast, during summer, biogenic sources—specifically the *isoprene oxidation products* and *monoterpenes* factors—played a more prominent role. The *isoprene oxidation products* contributed 36 % to the total OFP, compared to 9 % from monoterpenes. In the case of SOAP, the *monoterpenes factor* contributed 53 % of the overall SOAP during summer, while aromatic compounds contributed 29 %.

Comparing the total OFP between the two stations, BCN and MSY revealed similar values during the summer season, with 18.51 ppbv at BCN and 19.07 ppbv at MSY. However, during winter, the OFP was considerably lower at MSY, with 8.42 ppbv compared to 16.50 ppbv at BCN. On the other hand, the SOAP exhibited higher concentrations at BCN when compared to MSY, with 1.163 μg m^{-3} and 0.603 μg m^{-3} during winter at BCN and MSY, respectively, and 1.833 μg m^{-3} and 0.766 μg m^{-3} during summer at BCN and MSY, respectively.

While this study provides valuable insights into the sources of VOCs and their impacts on OFP and SOAP, some knowledge gaps should be acknowledged. First, both OFP and SOAP estimations are based on high nitrogen oxide (NO_x) environments, which may not accurately represent the low NO_x conditions at the MSY rural background station. Secondly, the biogenic contribution of monoterpenes is likely underestimated at BCN during summer due to their rapid oxidation by $OH^{\bullet}$ in an urban environment. Third, this study focused on a selection of 11 VOCs, and although they make substantial contributions to atmospheric concentrations, the inclusion of additional VOCs—particularly alkanes (~5–10 % contribution to OFP and SOAP) and alkenes (>30 % contribution to OFP)—would provide a more comprehensive understanding (Jookjantra et al., 2022; Wang et al., 2023; Wu et al., 2017; Yuan et al., 2009; Zhan et al., 2021). Finally, the study looked at the observed VOC mixing ratios and not the initial VOC mixing ratios before photochemical loss. This resulted in an underestimation of isoprene, monoterpenes, and the aromatic compounds. In relation to the OFP and SOAP estimation, this would result in higher contributions of these VOCs, and therefore should be considered in future research.

CRediT authorship contribution statement

Marten in 't Veld: Software, Validation, Formal analysis, Investigation, Writing – original draft, Writing – review & editing, Visualization. **Roger Seco:** Methodology, Validation, Formal analysis, Writing – review & editing. **Cristina Reche:** Validation, Data curation, Writing – review & editing. **Noemi Pérez:** Validation, Data curation, Writing – review & editing. **Andres Alastuey:** Conceptualization, Resources, Funding acquisition, Writing – review & editing. **Miguel Estrada-Portillo:** Resources, Writing – review & editing. **Ivan A. Janssens:** Resources, Writing – review & editing. **Josep Peñuelas:** Resources, Writing – review & editing. **Marcos Fernandez-Martinez:** Resources, Writing – review & editing. **Nicolas Marchand:** Resources, Formal analysis, Project administration, Funding acquisition, Supervision, Writing – review & editing. **Brice Temime-Roussel:** Resources, Validation, Formal analysis, Data curation, Validation, Writing – review & editing. **Xavier Querol:** Conceptualization, Resources, Project administration, Funding acquisition, Supervision, Writing – review & editing. **Ana Maria Yáñez-Serrano:** Conceptualization, Methodology, Software, Validation, Formal analysis, Investigation, Supervision, Funding acquisition, Writing – review & editing.

Declaration of competing interest

The authors declare that they have no known competing financial interests or personal relationships that could have appeared to influence the work reported in this paper.

Data availability

Data will be made available on request.

Acknowledgments

This study was supported by the European Union's Horizon 2020 research and innovation program under grant agreement 101036245 (RI-URBANS), the "Agencia Estatal de Investigación" from the Spanish Ministry of Science and Innovation, FEDER funds under the projects CAIAC (PID2019-108990RB-I00), the Generalitat de Catalunya (AGAUR 2021 SGR 00447), and the Direcció General de Territori. AMYS acknowledges a Ramón y Cajal grant (RYC2021-032519-I) and the La Caixa Foundation Junior Leader retaining fellowship. RS acknowledges a Ramón y Cajal grant (RYC2020-029216-I) funded by MCIN/AEI/ 10 .13039/501100011033 and by "ESF Investing in your future". IDAEA-CSIC is a Severo Ochoa Centre of Research Excellence (MCIN/AEI, Project CEX2018-000794-S). The authors thank the MASSALYA instrumental platform (Aix Marseille Université, lce.univ-amu.fr) for the analysis and measurements used in this work.

Appendix A. Supplementary data

Supplementary data to this article can be found online at https://doi.org/10.1016/j.scitotenv.2023.167159.

References

AIRUSE, 2016. Biomass Burning in Southern Europe.

Amato, F., Pandolfi, M., Escrig, A., Querol, X., Alastuey, A., Pey, J., Perez, N., Hopke, P. K., 2009. Quantifying road dust resuspension in urban environment by Multilinear Engine: a comparison with PMF2. Atmos. Environ. 43, 2770–2780. https://doi.org/10.1016/j.atmosenv.2009.02.039.

Amato, F., Alastuey, A., Karanasiou, A., Lucarelli, F., Nava, S., Calzolai, G., Severi, M., Becagli, S., Gianelle, V.L., Colombi, C., Alves, C., Custódio, D., Nunes, T., Cerqueira, M., Pio, C., Eleftheriadis, K., Diapouli, E., Reche, C., Minguillón, M.C., Manousakas, M.I., Maggos, T., Vratolis, S., Harrison, R.M., Querol, X., 2016. AIRUSE-LIFE+: a harmonized PM speciation and source apportionment in five southern European cities. Atmos. Chem. Phys. 16, 3289–3309. https://doi.org/10.5194/acp-16-3289-2016.

Arnold, S.R., Chipperfield, M.P., Blitz, M.A., Heard, D.E., Pilling, M.J., 2004. Photodissociation of acetone: atmospheric implications of temperature-dependent quantum yields. Geophys. Res. Lett. 31, 4–7. https://doi.org/10.1029/2003GL019099.

Atkinson, R., Arey, J., 2003. Atmospheric degradation of volatile organic compounds. Chem. Rev. 103, 4605–4638. https://doi.org/10.1021/cr0206420.

Atkinson, R., Carter, W.P.L., 1984. Kinetics and mechanisms of the gas-phase reactions of ozone with organic compounds under atmospheric conditions. Chem. Rev. 84, 437–470. https://doi.org/10.1021/cr00063a002.

Avnery, S., Mauzerall, D.L., Liu, J., Horowitz, L.W., 2011. Global crop yield reductions due to surface ozone exposure: 2. Year 2030 potential crop production losses and economic damage under two scenarios of O3 pollution. Atmos. Environ. 45, 2297–2309. https://doi.org/10.1016/j.atmosenv.2011.01.002.

Borbon, A., Veillerot, M., Locoge, N., Galloo, J., Guillermo, R., 2001. An investigation into the traffic-related fraction of isoprene at an urban location. Atmos. Environ. 35, 3749–3760. https://doi.org/10.1016/S1352-2310(01)00170-4.

Borbon, A., Locoge, N., Veillerot, M., Galloo, J.C., Guillermo, R., 2002. Characterisation of NMHCs in a French urban atmosphere: overview of the main sources. Sci. Total Environ. 292, 177–191. https://doi.org/10.1016/S0048-9697(01)01106-8.

Camredon, M., Aumont, B., Lee-Taylor, J., Madronich, S., 2007. The SOA/VOC/NOx system: an explicit model of secondary organic aerosol formation. Atmos. Chem. Phys. 7, 5599–5610.

Cerqueira, M., Gomes, L., Tarelho, L., Pio, C., 2013. Formaldehyde and acetaldehyde emissions from residential wood combustion in Portugal. Atmos. Environ. 72, 171–176. https://doi.org/10.1016/j.atmosenv.2013.02.045.

Chen, G., Liu, T., Ji, X., Xu, K., Hong, Y., Xu, L., Li, M., Fan, X., Chen, Y., Yang, C., Lin, Z., Huang, W., Chen, J., 2022. Source apportionment of VOCs and O3 production sensitivity at coastal and inland sites of Southeast China. Aerosol Air Qual. Res. 22 https://doi.org/10.4209/aaqr.220289.

Cui, L., Wu, D., Wang, S., Xu, Q., Hu, R., Hao, J., 2022. Measurement report: ambient volatile organic compound (VOC) pollution in urban Beijing: characteristics, sources, and implications for pollution control. Atmos. Chem. Phys. 22, 11931–11944. https://doi.org/10.5194/acp-22-11931-2022.

Cusack, M., Alastuey, A., Pérez, N., Pey, J., Querol, X., 2012. Trends of particulate matter (PM 2.5) and chemical composition at a regional background site in the Western Mediterranean over the last nine years (2002−2010). Atmos. Chem. Phys. 12, 8341–8357. https://doi.org/10.5194/acp-12-8341-2012.

de Gouw, J.A., Goldan, P.D., Warneke, C., Kuster, W.C., Roberts, J.M., Marchewka, M., Bertman, S.B., Pszenny, A.A.P., Keene, W.C., 2003. Validation of Proton Transfer Reaction-Mass Spectrometry (PTR-MS) Measurements of Gas-phase Organic Compounds in the Atmosphere during the New England Air Quality Study (NEAQS) in 2002, 108, pp. 1–18. https://doi.org/10.1029/2003JD003863.

Derwent, R.G., Jenkin, M.E., Utembe, S.R., Shallcross, D.E., Murrells, T.P., Passant, N.R., 2010. Secondary organic aerosol formation from a large number of reactive man-made organic compounds. Sci. Total Environ. 408, 3374–3381. https://doi.org/10.1016/j.scitotenv.2010.04.013.

Doerffel, K., 1984. Statistik in der analytischen Chemie. In: Verslag Chemie, pp. 51–72. Weinheim.

Drinovec, L., Močnik, G., Zotter, P., Prévôt, A.S.H., Ruckstuhl, C., Coz, E., Rupakheti, M., Sciare, J., Müller, T., Wiedensohler, A., Hansen, A.D.A., 2015. The "dual-spot" Aethalometer: an improved measurement of aerosol black carbon with real-time loading compensation. Atmos. Meas. Tech. 8, 1965–1979. https://doi.org/10.5194/amt-8-1965-2015.

Dunne, E., Galbally, I.E., Cheng, M., Selleck, P., Molloy, S.B., Lawson, S.J., 2018. Comparison of VOC measurements made by PTR-MS, adsorbent tubes-GC-FID-MS and DNPH derivatization-HPLC during the Sydney Particle Study, 2012: a contribution to the assessment of uncertainty in routine atmospheric VOC measurements. Atmos. Meas. Tech. 11, 141–159. https://doi.org/10.5194/amt-11-141-2018.

Ealo, M., Alastuey, A., Pérez, N., Ripoll, A., Querol, X., Pandolfi, M., 2018. Impact of aerosol particle sources on optical properties in urban, regional and remote areas in the north-western Mediterranean. Atmos. Chem. Phys. 18, 1149–1169. https://doi.org/10.5194/acp-18-1149-2018.

EC, 2008. DIRECTIVE 2008/50/EC of the european parliament and of the council of 21 May 2008 on ambient air quality and cleaner air for Europe. Off. J. Eur. Union 152, 44. https://eur-lex.europa.eu/legal-content/EN/TXT/?uri=celex%3A32008L0050.

EEA, 2015. Sulphur Dioxide (SO2) Emissions [WWW Document].

EEA, 2018a. Air quality in Europe — 2018 report. In: EEA Report No 12/2018. European Environmental Agency, Copenhagen. https://doi.org/10.2800/777411.

EEA, 2018b. Nitrogen Oxides (NOx) Emissions [WWW Document].

EEA, 2019. Air quality in Europe — 2019 report. In: EEA Report No 10/2019. European Environmental Agency, Copenhagen. https://doi.org/10.2800/822355.

EEA, 2021. Air quality in Europe 2021. https://doi.org/10.2800/549289.

EMEP/CCC, 2016. Air Pollution Trends in the EMEP Region Between 1990 and 2012. (EMEP: CCC-Report 1/2016). Norwegian Institute for Air Research, Kjeller.

Escrig, A., Monfort, E., Celades, I., Querol, X., Amato, F., Minguillón, M.C., Hopke, P.K., 2009. Application of optimally scaled target factor analysis for assessing source contribution of ambient PM10. J. Air Waste Manage. Assoc. 59, 1296–1307. https://doi.org/10.3155/1047-3289.59.11.1296.

Fall, R., Benson, A.A., 1996. Leaf methanol — the simplest natural product from plants. Trends Plant Sci. 1, 296–301. https://doi.org/10.1016/S1360-1385(96)88175-0.

Felzer, B.S., Cronin, T., Reilly, J.M., Melillo, J.M., Wang, X., 2007. Impacts of ozone on trees and crops. Compt. Rendus Geosci. 339, 784–798. https://doi.org/10.1016/j.crte.2007.08.008.

Fernández-Iriarte, A., Amato, F., Moreno, N., Pacitto, A., Reche, C., Marco, E., Grimalt, J. O., Querol, X., Moreno, T., 2020. Chemistry and sources of PM2.5 and volatile organic compounds breathed inside urban commuting and tourist buses. Atmos. Environ. 223 https://doi.org/10.1016/j.atmosenv.2019.117234.

Fernández-Martínez, M., Llusià, J., Filella, I., Niinemets, Ü., Arneth, A., Wright, I.J., Loreto, F., Peñuelas, J., 2018. Nutrient-rich plants emit a less intense blend of volatile isoprenoids. New Phytol. 220, 773–784. https://doi.org/10.1111/nph.14889.

Filella, I., Peñuelas, J., 2006. Daily, weekly, and seasonal time courses of VOC concentrations in a semi-urban area near Barcelona. Atmos. Environ. 40, 7752–7769. https://doi.org/10.1016/j.atmosenv.2006.08.002.

Gangoiti, G., Alonso, L., Navazo, M., Albizuri, A., Perez-Landa, G., Matabuena, M., Valdenebro, V., Maruri, M., Antonio García, J., Millán, M.M., 2001. Regional transport of pollutants over the Bay of Biscay: analysis of an ozone episode under a blocking anticyclone in west-central Europe. Atmos. Environ. 36, 1349–1361. https://doi.org/10.1016/S1352-2310(01)00536-2.

Gelencsér, A., Siszler, K., Hlavay, J., 1997. Toluene-Benzene Concentration Ratio as a Tool for Characterizing the Distance from Vehicular Emission Sources.

Gómez, M.C., Durana, N., García, J.A., de Blas, M., Sáez de Cámara, E., García-Ruiz, E., Gangoiti, G., Torre-Pascual, E., Iza, J., 2020. Long-term measurement of biogenic volatile organic compounds in a rural background area: contribution to ozone formation. Atmos. Environ. 224 https://doi.org/10.1016/j.atmosenv.2020.117315.

Graus, M., Müller, M., Hansel, A., 2010. High Resolution PTR-TOF: Quantification and Formula Confirmation of VOC in Real Time, 21. American Society for Mass Spectrometry, pp. 1037–1044.

Gu, S., Guenther, A., Faiola, C., 2021. Effects of anthropogenic and biogenic volatile organic compounds on Los Angeles air quality. Environ. Sci. Technol. https://doi.org/10.1021/acs.est.1c01481.

Gu, Y., Liu, B., Meng, H., Song, S., Dai, Q., Shi, L., Feng, Y., Hopke, P.K., 2023. Source apportionment of consumed volatile organic compounds in the atmosphere. J. Hazard. Mater. 459. https://doi.org/10.1016/j.jhazmat.2023.132138.

Gueneron, M., Erickson, M.H., Vanderschelden, G.S., Jobson, B.T., 2015. PTR-MS fragmentation patterns of gasoline hydrocarbons. Int. J. Mass Spectrom. 379, 97–109. https://doi.org/10.1016/j.ijms.2015.01.001.

Harrison, D., Hunter, M.C., Lewis, A.C., Seakins, P.W., Bonsang, B., Gros, V., Kanakidou, M., Touaty, M., Kavouras, I., Mihalopoulos, N., Stephanou, E., Alves, C., Nunes, T., Pio, C., 2001. Ambient isoprene and monoterpene concentrations in a Greek fir (Abies Borisii-regis) forest. Reconciliation with emissions measurements and effects on measured OH concentrations. Atmos. Environ. 35, 4699–4711. https://doi.org/10.1016/S1352-2310(01)00091-7.

Heeb, N.V., Forss, A.-M., Bach, C., Reimann, S., Herzog, A., Jäckle, H.W., 2000. A comparison of benzene, toluene and C2-benzenes mixing ratios in automotive exhaust and in the suburban atmosphere during the introduction of catalytic converter technology to the Swiss Car Fleet. Atmos. Environ. 34, 3103–3116. https://doi.org/10.1016/S1352-2310(99)00446-X.

Heiden, M.G.V., Cantley, L.C., Thompson, C.B., 2009. Understanding the Warburg effect: the metabolic requirements of cell proliferation. Science 1979. https://doi.org/10.1126/science.1160809.

Hellén, H., Hakola, H., Reissell, A., Ruuskanen, T.M., 2004. Atmospheric chemistry and physics carbonyl compounds in boreal coniferous forest air in Hyytiälä, Southern Finland. Atmos. Chem. Phys. 4, 1771–1780.

Hellén, H., Tykkä, T., Hakola, H., 2012. Importance of monoterpenes and isoprene in urban air in northern Europe. Atmos. Environ. 59, 59–66. https://doi.org/10.1016/j.atmosenv.2012.04.049.

Holzinger, R., Wameke, C., Hansel, A., Jordan, A., Lindinger, W., Scharffe, D.H., Schade, G., Crutzen, P.J., 1999. Biomass burning as a source of formaldehyde, acetaldehyde, methanol, acetone, acetonitrile, and hydrogen cyanide. Geophys. Res. Lett. 26, 1161–1164. https://doi.org/10.1029/1999GL900156.

Holzinger, R., Sandoval-Soto, L., Rottenberger, S., Crutzen, P.J., Kesselmeier, J., 2000. Emissions of volatile organic compounds from Quercus ilex L. measured by Proton Transfer Reaction Mass Spectrometry under different environmental conditions. J. Geophys. Res. Atmos. 105, 20573–20579. https://doi.org/10.1029/2000JD900296.

Holzinger, R., Williams, J., Salisbury, G., Kï Upfel, T., De Reus, M., Traub, M., Crutzen, P. J., Lelieveld, J., 2005. Oxygenated compounds in aged biomass burning plumes over the Eastern Mediterranean: evidence for strong secondary production of methanol and acetone. Atmos. Chem. Phys. 5, 39–46.

Hüve, K., Christ, M., Kleist, E., Uerlings, R., Niinemets, Ü., Walter, A., Wildt, J., 2007. Simultaneous growth and emission measurements demonstrate an interactive control of methanol release by leaf expansion and stomata. J. Exp. Bot. 58, 1783–1793. https://doi.org/10.1093/jxb/erm038.

in 't Veld, M., Alastuey, A., Pandolfi, M., Amato, F., Pérez, N., Reche, C., Via, M., Minguillón, M.C., Escudero, M., Querol, X., 2021. Compositional changes of PM2.5 in NE Spain during 2009–2018: a trend analysis of the chemical composition and source apportionment. Sci. Total Environ. 795 https://doi.org/10.1016/j.scitotenv.2021.148728.

in 't Veld, M., Pandolfi, M., Amato, F., Pérez, N., Reche, C., Dominutti, P., Jaffrezo, J., Alastuey, A., Querol, X., Uzu, G., 2023. Discovering oxidative potential (OP) drivers of atmospheric PM10, PM2.5, and PM1 simultaneously in North-Eastern Spain. Sci. Total Environ. 857 https://doi.org/10.1016/j.scitotenv.2022.159386.

Ionicon Analytik GmbH, 2014. Fundamentals of PTR-MS.

Jacob, D.J., 1999a. Chapter 11: oxidising power of the troposphere. In: Introduction to Atmospheric Chemistry. Princeton University Press, pp. 199–219. https://doi.org/10.1111/j.0954-6820.1949.tb11329.x.

Jacob, D.J., 1999b. Chapter 12: ozone air pollution. In: Introduction to Atmospheric Chemistry. Princeton University Press, pp. 232–243. https://doi.org/10.1111/j.0954-6820.1949.tb11329.x.

Jacob, D.J., 1999c. Chapter 8: aerosols. In: Introduction to Atmospheric Chemistry. Princeton University Press, pp. 144–152. https://doi.org/10.1111/j.0954-6820.1949.tb11329.x.
Jiménez, P., Parra, R., Gassó, S., Baldasano, J.M., 2005. Modeling the ozone weekend effect in very complex terrains: a case study in the Northeastern Iberian Peninsula. Atmos. Environ. 39, 429–444. https://doi.org/10.1016/j.atmosenv.2004.09.065.
Jookjantra, P., Thepanondh, S., Keawboonchu, J., Kultan, V., Laowagul, W., 2022. Formation potential and source contribution of secondary organic aerosol from volatile organic compounds. J. Environ. Qual. 51, 1016–1034. https://doi.org/10.1002/jeq2.20381.
Juráň, S., Pallozzi, E., Guidolotti, G., Fares, S., Šigut, L., Calfapietra, C., Alivernini, A., Savi, F., Večeřová, K., Křůmal, K., Večeřa, Z., Urban, O., 2017. Fluxes of biogenic volatile organic compounds above temperate Norway spruce forest of the Czech Republic. Agric. For. Meteorol. 232, 500–513. https://doi.org/10.1016/j.agrformet.2016.10.005.
Karl, T., Hansel, A., Cappellin, L., Kaser, L., Herdlinger-Blatt, I., Jud, W., 2012. Selective measurements of isoprene and 2-methyl-3-buten-2-ol based on NO+ ionization mass spectrometry. Atmos. Chem. Phys. 12, 11877–11884. https://doi.org/10.5194/acp-12-11877-2012.
Kaser, L., Karl, T., Guenther, A., Graus, M., Schnitzhofer, R., Turnipseed, A., Fischer, L., Harley, P., Madronich, M., Gochis, D., Keutsch, F.N., Hansel, A., 2013. Undisturbed and disturbed above canopy ponderosa pine emissions: PTR-TOF-MS measurements and MEGAN 2.1 model results. Atmos. Chem. Phys. 13, 11935–11947. https://doi.org/10.5194/acp-13-11935-2013.
Khoder, M.I., 2007. Ambient levels of volatile organic compounds in the atmosphere of Greater Cairo. Atmos. Environ. 41, 554–566. https://doi.org/10.1016/j.atmosenv.2006.08.051.
Krupa, S.V., Manning, W.J., 1988. Atmospheric ozone: formation and effects on vegetation. Environ. Pollut. 50, 101–137.
Kumar, A., Singh, D., Kumar, K., Singh, B.B., Jain, V.K., 2018. Distribution of VOCs in urban and rural atmospheres of subtropical India: temporal variation, source attribution, ratios, OFP and risk assessment. Sci. Total Environ. 613–614, 492–501. https://doi.org/10.1016/j.scitotenv.2017.09.096.
Langford, B., Davison, B., Nemitz, E., Hewitt, C.N., 2009. Mixing ratios and eddy covariance flux measurements of volatile organic compounds from an urban canopy (Manchester, UK). Atmos. Chem. Phys. 9, 1971–1987. https://doi.org/10.5194/acp-9-1971-2009.
Lewis, A.C., Hopkins, J.R., Carpenter, L.J., Stanton, J., Read, K.A., Pilling, M.J., 2005. Sources and sinks of acetone, methanol, and acetaldehyde in North Atlantic marine air. Atmos. Chem. Phys. 5, 1963–1974. https://doi.org/10.5194/acp-5-1963-2005.
Li, L., Chen, Y., Zeng, L., Shao, M., Xie, S., Chen, W., Lu, S., Wu, Y., Cao, W., 2014. Biomass burning contribution to ambient volatile organic compounds (VOCs) in the Chengdu-Chongqing region (CCR), China. Atmos. Environ. 99, 403–410. https://doi.org/10.1016/j.atmosenv.2014.09.067.
Li, M., Li, Q., Nantz, M.H., Fu, X.A., 2018. Analysis of carbonyl compounds in ambient air by a microreactor approach. ACS Omega 3, 6764–6769. https://doi.org/10.1021/acsomega.8b00503.
Ling, Z., He, Z., Wang, Z., Shao, M., Wang, X., 2019. Sources of methacrolein and methyl vinyl ketone and their contributions to methylglyoxal and formaldehyde at a receptor site in Pearl River Delta. J. Environ. Sci. 79, 1–10. https://doi.org/10.1016/j.jes.2018.12.001.
Liu, Y., Shao, M., Fu, L., Lu, S., Zeng, L., Tang, D., 2008. Source profiles of volatile organic compounds (VOCs) measured in China: part I. Atmos. Environ. 42, 6247–6260. https://doi.org/10.1016/j.atmosenv.2008.01.070.
Liu, Y.J., Herdlinger-Blatt, I., McKinney, K.A., Martin, S.T., 2013. Production of methyl vinyl ketone and methacrolein via the hydroperoxyl pathway of isoprene oxidation. Atmos. Chem. Phys. 13, 5715–5730. https://doi.org/10.5194/acp-13-5715-2013.
Liu, B., Yang, Y., Yang, T., Dai, Q., Zhang, Y., Feng, Y., Hopke, P.K., 2023. Effect of photochemical losses of ambient volatile organic compounds on their source apportionment. Environ. Int. 172 https://doi.org/10.1016/j.envint.2023.107766.
Louie, P.K.K., Ho, J.W.K., Tsang, R.C.W., Blake, D.R., Lau, A.K.H., Yu, J.Z., Yuan, Z., Wang, X., Shao, M., Zhong, L., 2013. VOCs and OVOCs distribution and control policy implications in Pearl River Delta region, China. Atmos. Environ. 76, 125–135. https://doi.org/10.1016/j.atmosenv.2012.08.058.
Luecken, D.J., Hutzell, W.T., Strum, M.L., Pouliot, G.A., 2012. Regional sources of atmospheric formaldehyde and acetaldehyde, and implications for atmospheric modeling. Atmos. Environ. 47, 477–490. https://doi.org/10.1016/j.atmosenv.2011.10.005.
Luo, W., Wang, B., Liu, S., 2011. VOC ozone formation potential and emission sources in the atmosphere of Guangzhou. Environ. Sci. Technol. 34, 80–86.
Luo, H., Li, G., Chen, J., Lin, Q., Ma, S., Wang, Y., An, T., 2020. Spatial and temporal distribution characteristics and ozone formation potentials of volatile organic compounds from three typical functional areas in China. Environ. Res. 183 https://doi.org/10.1016/j.envres.2020.109141.
Millán, M.M., 2014. Extreme hydrometeorological events and climate change predictions in Europe. J. Hydrol. (Amst) 518, 206–224. https://doi.org/10.1016/j.jhydrol.2013.12.041.
Millán, M.M., Salvador, R., Mantilla, E., Kallos, G., 1997. Photooxidant dynamics in the Mediterranean basin in summer: results from European research projects. J. Geophys. Res. 102, 8811–8823. https://doi.org/10.1029/96jd03610.
Millán, M.M., José Sanz, M., Salvador, R., Mantilla, E., 2002. Atmospheric dynamics and ozone cycles related to nitrogen deposition in the western Mediterranean. Environ. Pollut. 118, 167–186. https://doi.org/10.1016/S0269-7491(01)00311-6.
Misztal, P.K., Hewitt, C.N., Wildt, J., Blande, J.D., Eller, A.S.D., Fares, S., Gentner, D.R., Gilman, J.B., Graus, M., Greenberg, J., Guenther, A.B., Hansel, A., Harley, P., Huang, M., Jardine, K., Karl, T., Kaser, L., Keutsch, F.N., Kiendler-Scharr, A., Kleist, E., Lerner, B.M., Li, T., Mak, J., Nölscher, A.C., Schnitzhofer, R., Sinha, V., Thornton, B., Warneke, C., Wegener, F., Werner, C., Williams, J., Worton, D.R., Yassaa, N., Goldstein, A.H., 2015. Atmospheric benzenoid emissions from plants rival those from fossil fuels. Sci. Rep. 5 https://doi.org/10.1038/srep12064.
Möller, D., 2004. The tropospheric ozone problem. Arh. Hig. Rada Toksikol. 55, 11–23.
Nogueira, T., de Souza, K.F., Fornaro, A., Andrade, M. de F., de Carvalho, L.R.F., 2015. On-road emissions of carbonyls from vehicles powered by biofuel blends in traffic tunnels in the Metropolitan Area of Sao Paulo, Brazil. Atmos. Environ. 108, 88–97. https://doi.org/10.1016/j.atmosenv.2015.02.064.
Norris, G., Duvall, R., Brown, S., Bai, S., 2014. EPA Positive Matrix Factorization (PMF) 5.0 Fundamentals and User Guide [WWW Document]. EPA.
Pacifico, F., Harrison, S.P., Jones, C.D., Arneth, A., Sitch, S., Weedon, G.P., Barkley, M.P., Palmer, P.I., Serça, D., Potosnak, M., Fu, T.-M., Goldstein, A., Bai, J., Schurgers, G., 2011. Evaluation of a photosynthesis-based biogenic isoprene emission scheme in JULES and simulation of isoprene emissions under present-day climate conditions. Atmos. Chem. Phys. 11, 4371–4389. https://doi.org/10.5194/acp-11-4371-2011.
Pagès, A.B., Peñuelas, J., Clarà, J., Llusià, J., López, F.C.I., Maneja, R., 2020. How should forests be characterized in regard to human health? Evidence from existing literature. Int. J. Environ. Res. Public Health. https://doi.org/10.3390/ijerph17031027.
Pandolfi, M., Martucci, G., Querol, X., Alastuey, A., Wilsenack, F., Frey, S., O'Dowd, C.D., Dall'Osto, M., 2013. Continuous atmospheric boundary layer observations in the coastal urban area of Barcelona during SAPUSS. Atmos. Chem. Phys. 13, 4983–4996. https://doi.org/10.5194/acp-13-4983-2013.
Pandolfi, M., Querol, X., Alastuey, A., Jimenez, J.L., Jorba, O., Day, D., Ortega, A., Cubison, M.J., Comerón, A., Sicard, M., Mohr, C., Prevot, A.S.H., Minguillón, M.C., Pey, J., Baldasano, J.M., Burkhart, J.F., Seco, R., Peñuelas, J., van Drooge, B.L., Artiñano, B., Di Marco, C., Nemitz, E., Schallhart, S., Metzger, A., Hansel, A., Lorente, J., Ng, S., Jayne, J., Szidat, S., 2014. Effects of sources and meteorology on particulate matter in the Western Mediterranean Basin: an overview of the DAURE campaign. J. Geophys. Res. 119, 4978–5010. https://doi.org/10.1002/2013JD021079.
Pandolfi, M., Alastuey, A., Pérez, N., Reche, C., Castro, I., Shatalov, V., Querol, X., 2016. Trends analysis of PM source contributions and chemical tracers in NE Spain during 2004-2014: a multi-exponential approach. Atmos. Chem. Phys. 16, 11787–11805. https://doi.org/10.5194/acp-16-11787-2016.
Paoletti, E., De Marco, A., Beddows, D.C.S., Harrison, R.M., Manning, W.J., 2014. Ozone levels in European and USA cities are increasing more than at rural sites, while peak values are decreasing. Environ. Pollut. 192, 295–299. https://doi.org/10.1016/j.envpol.2014.04.040.
Peñuelas, J., Filella, I., Seco, R., Llusià, J., 2009. Increase in isoprene and monoterpene emissions after re-watering of droughted Quercus ilex seedlings. Biol. Plant. 53, 351–354. https://doi.org/10.1007/s10535-009-0065-4.
Pérez, C., Sicard, M., Jorba, O., Comerón, A., Baldasano, J.M., 2004. Summertime re-circulations of air pollutants over the north-eastern Iberian coast observed from systematic EARLINET lidar measurements in Barcelona. Atmos. Environ. 38, 3983–4000. https://doi.org/10.1016/j.atmosenv.2004.04.010.
Pérez, N., Pey, J., Castillo, S., Viana, M., Alastuey, A., Querol, X., 2008. Interpretation of the variability of levels of regional background aerosols in the Western Mediterranean. Sci. Total Environ. 407, 527–540. https://doi.org/10.1016/j.scitotenv.2008.09.006.
Pérez, N., Pey, J., Reche, C., Cortés, J., Alastuey, A., Querol, X., 2016. Impact of harbour emissions on ambient PM10 and PM2.5 in Barcelona (Spain): evidences of secondary aerosol formation within the urban area. Sci. Total Environ. 571, 237–250. https://doi.org/10.1016/j.scitotenv.2016.07.025.
Pey, J., Querol, X., Alastuey, A., 2009. Variations of levels and composition of PM10 and PM2.5 at an insular site in the Western Mediterranean. Atmos. Res. 94, 285–299. https://doi.org/10.1016/j.atmosres.2009.06.006.
Pinthong, N., Thepanondh, S., Kondo, A., 2022. Source identification of VOCs and their environmental health risk in a petrochemical industrial area. Aerosol Air Qual. Res. 22 https://doi.org/10.4209/aaqr.210064.
Possanzini, M., Di Palo, V., Cecinato, A., 2002. Sources and photodecomposition of formaldehyde and acetaldehyde in Rome ambient air. Atmos. Environ. 36, 3195–3201. https://doi.org/10.1016/S1352-2310(02)00192-9.
Querol, X., Alastuey, A., Rodriguez, S., Plana, F., Ruiz, C.R., Cots, N., Massagué, G., Puig, O., 2001. PM10 and PM2.5 source apportionment in the Barcelona Metropolitan area, Catalonia, Spain. Atmos. Environ. 35, 6407–6419. https://doi.org/10.1016/S1352-2310(01)00361-2.
Querol, X., Alastuey, A., Ruiz, C.R., Artiñano, B., Hansson, H.C., Harrison, R.M., Buringh, E., Ten Brink, H.M., Lutz, M., Bruckmann, P., Straehl, P., Schneider, J., 2004a. Speciation and origin of PM10 and PM2.5 in selected European cities. Atmos. Environ. 38, 6547–6555. https://doi.org/10.1016/j.atmosenv.2004.08.037.
Querol, X., Alastuey, A., Viana, M.M., Rodriguez, S., Artiñano, B., Salvador, P., Garcia Do Santos, S., Fernandez Patier, R., Ruiz, C.R., De La Rosa, J., Sanchez De La Campa, A., Menendez, M., Gil, J.I., 2004b. Speciation and origin of PM10 and PM2.5 in Spain. J. Aerosol Sci. 35, 1151–1172. https://doi.org/10.1016/j.jaerosci.2004.04.002.
Querol, X., Alastuey, A., Pandolfi, M., Reche, C., Pérez, N., Minguillón, M.C., Moreno, T., Viana, M., Escudero, M., Orio, A., Pallarés, M., Reina, F., 2014. 2001-2012 trends on air quality in Spain. Sci. Total Environ. 490, 957–969. https://doi.org/10.1016/j.scitotenv.2014.05.074.
Querol, X., Alastuey, A., Reche, C., Orio, A., Pallares, M., Reina, F., Dieguez, J.J., Mantilla, E., Escudero, M., Alonso, L., Gangoiti, G., Millán, M., 2016. On the origin of the highest ozone episodes in Spain. Sci. Total Environ. 572, 379–389. https://doi.org/10.1016/j.scitotenv.2016.07.193.
Querol, X., Gangoiti, G., Mantilla, E., Alastuey, A., Minguillón, M.C., Amato, F., Reche, C., Viana, M., Moreno, T., Karanasiou, A., Rivas, I., Pérez, N., Ripoll, A.,

Brines, M., Ealo, M., Pandolfi, M., Lee, H.K., Eun, H.R., Park, Y.H., Escudero, M., Beddows, D., Harrison, R.M., Bertrand, A., Marchand, N., Lyasota, A., Codina, B., Olid, M., Udina, M., Jiménez-Esteve, B., Jiménez-Esteve, B.B., Alonso, L., Millán, M., Ahn, K.H., 2017. Phenomenology of high-ozone episodes in NE Spain. Atmos. Chem. Phys. 17, 2817–2838. https://doi.org/10.5194/acp-17-2817-2017.

Querol, X., Alastuey, A., Gangoiti, G., Perez, N., Lee, H.K., Eun, H.R., Park, Y., Mantilla, E., Escudero, M., Titos, G., Alonso, L., Temime-Roussel, B., Marchand, N., Moreta, J.R., Revuelta, M.A., Salvador, P., Artíñano, B., Dos Santos, S.G., Anguas, M., Notario, A., Saiz-Lopez, A., Harrison, R.M., Millán, M., Ahn, K.H., 2018. Phenomenology of summer ozone episodes over the Madrid Metropolitan Area, central Spain. Atmos. Chem. Phys. 18, 6511–6533. https://doi.org/10.5194/acp-18-6511-2018.

Reche, C., Viana, M., Amato, F., Alastuey, A., Moreno, T., Hillamo, R., Teinilä, K., Saarnio, K., Seco, R., Peñuelas, J., Mohr, C., Prévôt, A.S.H., Querol, X., 2012. Biomass burning contributions to urban aerosols in a coastal Mediterranean City. Sci. Total Environ. 427–428, 175–190. https://doi.org/10.1016/j.scitotenv.2012.04.012.

Ripoll, A., Minguillón, M.C., Pey, J., Pérez, N., Querol, X., Alastuey, A., 2015. Joint analysis of continental and regional background environments in the western Mediterranean: PM1 and PM10 concentrations and composition. Atmos. Chem. Phys. 15, 1129–1145. https://doi.org/10.5194/acp-15-1129-2015.

Saiz-Lopez, A., Borge, R., Notario, A., Adame, J.A., Paz, D.D. La, Querol, X., Artíñano, B., Gómez-Moreno, F.J., Cuevas, C.A., 2017. Unexpected increase in the oxidation capacity of the urban atmosphere of Madrid, Spain. Sci. Rep. 7, 1–11. https://doi.org/10.1038/srep45956.

Sanadze, G.A., 2004. Biogenic isoprene (a review). Russ. J. Plant Physiol. 51, 729–741. https://doi.org/10.1023/B:RUPP.0000047821.63354.a4.

Sanhueza, E., Holzinger, R., Kleiss, B., Donoso, L., Crutzen, P.J., 2004. Atmospheric chemistry and physics new insights in the global cycle of acetonitrile: release from the ocean and dry deposition in the tropical savanna of Venezuela. Atmos. Chem. Phys. 4, 275–280.

Seco, R., Peñuelas, J., Filella, I., 2007. Short-chain oxygenated VOCs: emission and uptake by plants and atmospheric sources, sinks, and concentrations. Atmos. Environ. https://doi.org/10.1016/j.atmosenv.2006.11.029.

Seco, R., Peñuelas, J., Filella, I., Llusià, J., Molowny-Horas, R., Schallhart, S., Metzger, A., Müller, M., Hansel, A., 2011. Contrasting winter and summer VOC mixing ratios at a forest site in the Western Mediterranean Basin: the effect of local biogenic emissions. Atmos. Chem. Phys. 11, 13161–13179. https://doi.org/10.5194/acp-11-13161-2011.

Seco, R., Peñuelas, J., Filella, I., Llusia, J., Schallhart, S., Metzger, A., Müller, M., Hansel, A., 2013. Volatile organic compounds in the western Mediterranean basin: Urban and rural winter measurements during the DAURE campaign. Atmos. Chem. Phys. 13, 4291–4306. https://doi.org/10.5194/acp-13-4291-2013.

Seinfeld, J.I., Pandis, S.N., 2016. Atmospheric Chemistry and Physics: From Air Pollution to Climate Change, 3rd edition. Wiley. https://doi.org/10.1080/00139157.1999.10544295.

Singh, H.B., O'Hara, D., Herlth, D., Sachse, W., Blake, D.R., Bradshaw, J.D., Kanakidou, M., Crutzen, P.J., 1994. Acetone in the atmosphere: distribution, sources, and sinks. J. Geophys. Res. 99, 1805. https://doi.org/10.1029/93jd00764.

Sinharoy, P., McAllister, S.L., Vasu, M., Gross, E.R., 2019. Environmental aldehyde sources and the health implications of exposure. In: Advances in Experimental Medicine and Biology. Springer New York LLC, pp. 35–52. https://doi.org/10.1007/978-981-13-6260-6_2.

Sjostedt, S.J., Leaitch, W.R., Levasseur, M., Scarratt, M., Michaud, S., Motard-Cté, J., Burkhart, J.H., Abbatt, J.P.D., 2012. Evidence for the uptake of atmospheric acetone and methanol by the Arctic Ocean during late summer DMS-Emission plumes. J. Geophys. Res. 117, 1–15. https://doi.org/10.1029/2011JD017086.

Stevenson, D.S., Dentener, F.J., Schultz, M.G., Ellingsen, K., van Noije, T.P.C., Wild, O., Zeng, G., Amann, M., Atherton, C.S., Bell, N., Bergmann, D.J., Bey, I., Butler, T., Cofala, J., Collins, W.J., Derwent, R.G., Doherty, R.M., Drevet, J., Eskes, H.J., Fiore, A.M., Gauss, M., Hauglustaine, D.A., Horowitz, L.W., Isaksen, I.S.A., Krol, M. C., Lamarque, J.F., Lawrence, M.G., Montanaro, V., Müller, J.F., Pitari, G., Prather, M.J., Pyle, J.A., Rast, S., Rodriquez, J.M., Sanderson, M.G., Savage, N.H., Shindell, D.T., Strahan, S.E., Sudo, K., Szopa, S., 2006. Multimodel ensemble simulations of present-day and near-future tropospheric ozone. J. Geophys. Res. 111 https://doi.org/10.1029/2005JD006338.

Stroud, C.A., Roberts, J.M., Goldan, P.D., Kuster, W.C., Murphy, P.C., Williams, E.J., Hereid, D., Parrish, D., Sueper, D., Trainer, M., Fehsenfeld, F.C., Apel, E.C., Riemer, D., Wert, B., Henry, B., Fried, A., Martinez-Harder, M., Harder, H., Brune, W. H., Li, G., Xie, H., Young, V.L., 2001. Isoprene and its oxidation products, methacrolein and methylvinyl ketone, at an urban forested site during the 1999: southern oxidants study. J. Geophys. Res. Atmos. 106, 8035–8046. https://doi.org/10.1029/2000JD900628.

Tan, Y., Han, S., Chen, Y., Zhang, Z., Li, H., Li, W., Yuan, Q., Li, X., Wang, T., Lee, Cheng, S., 2021. Characteristics and source apportionment of volatile organic compounds (VOCs) at a coastal site in Hong Kong. Sci. Total Environ. 777 https://doi.org/10.1016/j.scitotenv.2021.146241.

Venecek, M.A., Carter, W.P.L., Kleeman, M.J., 2018. Updating the SAPRC Maximum Incremental Reactivity (MIR) scale for the United States from 1988 to 2010. J. Air Waste Manage. Assoc. 68, 1301–1316. https://doi.org/10.1080/10962247.2018.1498410.

Via, M., Minguillón, M.C., Reche, C., Querol, X., Alastuey, A., 2021. Increase of secondary organic aerosol over four years in an urban environment. Atmos. Chem. Phys. 21, 8323–8339. https://doi.org/10.5194/acp-21-8323-2021.

Viana, M., Reche, C., Amato, F., Alastuey, A., Querol, X., Moreno, T., Lucarelli, F., Nava, S., Calzolai, G., Chiari, M., Rico, M., 2013. Evidence of biomass burning aerosols in the Barcelona urban environment during winter time. Atmos. Environ. 72, 81–88. https://doi.org/10.1016/j.atmosenv.2013.02.031.

Viskari, E.-L., Vartiainen, M., Pasanen, P., 2000. Seasonal and diurnal variation in formaldehyde and acetaldehyde concentrations along a highway in Eastern Finland. Atmos. Environ. 34, 917–923. https://doi.org/10.1016/S1352-2310(99)00307-6.

Wagner, P., Kuttler, W., 2014. Biogenic and anthropogenic isoprene in the near-surface urban atmosphere - a case study in Essen, Germany. Sci. Total Environ. 475, 104–115. https://doi.org/10.1016/j.scitotenv.2013.12.026.

Wang, B., Li, Z., Liu, Z., Sun, Y., Wang, C., Xiao, Y., Lu, X., Yan, G., Xu, C., 2023. Characteristics, secondary transformation potential and health risks of atmospheric volatile organic compounds in an industrial area in Zibo, East China. Atmosphere (Basel) 14, 158. https://doi.org/10.3390/atmos14010158.

Warneke, C., Veres, P., Holloway, J.S., Stutz, J., Tsai, C., Alvarez, S., Rappenglueck, B., Fehsenfeld, F.C., Graus, M., Gilman, J.B., De Gouw, J.A., 2011. Airborne formaldehyde measurements using PTR-MS: calibration, humidity dependence, inter-comparison and initial results. Atmos. Meas. Tech. 4, 2345–2358. https://doi.org/10.5194/amt-4-2345-2011.

Wu, W., Zhao, B., Wang, S., Hao, J., 2017. Ozone and secondary organic aerosol formation potential from anthropogenic volatile organic compounds emissions in China. J. Environ. Sci. (China) 53, 224–237. https://doi.org/10.1016/j.jes.2016.03.025.

Wu, Y., Fan, X., Liu, Y., Zhang, J., Wang, H., Sun, L., Fang, T., Mao, H., Hu, J., Wu, L., Peng, J., Wang, S., 2023. Source apportionment of VOCs based on photochemical loss in summer at a suburban site in Beijing. Atmos. Environ. 293. https://doi.org/10.1016/j.atmosenv.2022.119459.

Xu, J., Niehoff, N.M., White, A.J., Werder, E.J., Sandler, D.P., 2022. Fossil-fuel and combustion-related air pollution and hypertension in the Sister Study. Environ. Pollut. 315. https://doi.org/10.1016/j.envpol.2022.120401.

Yáñez-Serrano, A.M., Bach, A., Bartolomé-Català, D., Matthaios, V., Seco, R., Llusià, J., Filella, I., Peñuelas, J., 2021a. Dynamics of volatile organic compounds in a western Mediterranean oak forest. Atmos. Environ. 257 https://doi.org/10.1016/j.atmosenv.2021.118447.

Yáñez-Serrano, A.M., Filella, I., LLusià, J., Gargallo-Garriga, A., Granda, V., Bourtsoukidis, E., Williams, J., Seco, R., Cappellin, L., Werner, C., de Gouw, J., Peñuelas, J., 2021b. GLOVOCS - master compound assignment guide for proton transfer reaction mass spectrometry users. Atmos. Environ. 244 https://doi.org/10.1016/j.atmosenv.2020.117929.

Yang, T., Liu, B., Yang, Y., Dai, Q., Zhang, Y., Feng, Y., Hopke, P.K., 2022. Improved positive matrix factorization for source apportionment of volatile organic compounds in vehicular emissions during the Spring Festival in Tianjin, China. Environ. Pollut. 303 https://doi.org/10.1016/j.envpol.2022.119122.

Yee, L.D., Isaacman-Vanwertz, G., Wernis, R.A., Kreisberg, N.M., Glasius, M., Riva, M., Surratt, J.D., De Sá, S.S., Martin, S.T., Alexander, M.L., Palm, B.B., Hu, W., Campuzano-Jost, P., Day, D.A., Jimenez, J.L., Liu, Y., Misztal, P.K., Artaxo, P., Viegas, J., Manzi, A., De Souza, R.A.F., Edgerton, E.S., Baumann, K., Goldstein, A.H., 2020. Natural and anthropogenically influenced isoprene oxidation in southeastern United States and Central Amazon. Environ. Sci. Technol. 54, 5980–5991. https://doi.org/10.1021/acs.est.0c00805.

Young, P.J., Archibald, A.T., Bowman, K.W., Lamarque, J.-F., Naik, V., Stevenson, D.S., Tilmes, S., Voulgarakis, A., Wild, O., Bergmann, D., Cameron-Smith, P., Cionni, I., Collins, W.J., Dalsøren, S.B., Doherty, R.M., Eyring, V., Faluvegi, G., Horowitz, L.W., Josse, B., Lee, Y.H., MacKenzie, I.A., Nagashima, T., Plummer, D.A., Righi, M., Rumbold, S.T., Skeie, R.B., Shindell, D.T., Strode, S.A., Sudo, K., Szopa, S., Zeng, G., 2013. Pre-industrial to end 21st century projections of tropospheric ozone from the Atmospheric Chemistry and Climate Model Intercomparison Project (ACCMIP). Atmos. Chem. Phys. 13, 2063–2090. https://doi.org/10.5194/acp-13-2063-2013.

Yuan, Z., Lau, A.K.H., Shao, M., Louie, P.K.K., Liu, S.C., Zhu, T., 2009. Source analysis of volatile organic compounds by positive matrix factorization in urban and rural environments in Beijing. J. Geophys. Res. 114 https://doi.org/10.1029/2008JD011190.

Zhan, J., Feng, Z., Liu, P., He, X., He, Z., Chen, T., Wang, Y., He, H., Mu, Y., Liu, Y., 2021. Ozone and SOA formation potential based on photochemical loss of VOCs during the Beijing summer. Environ. Pollut. 285. https://doi.org/10.1016/j.envpol.2021.117444.